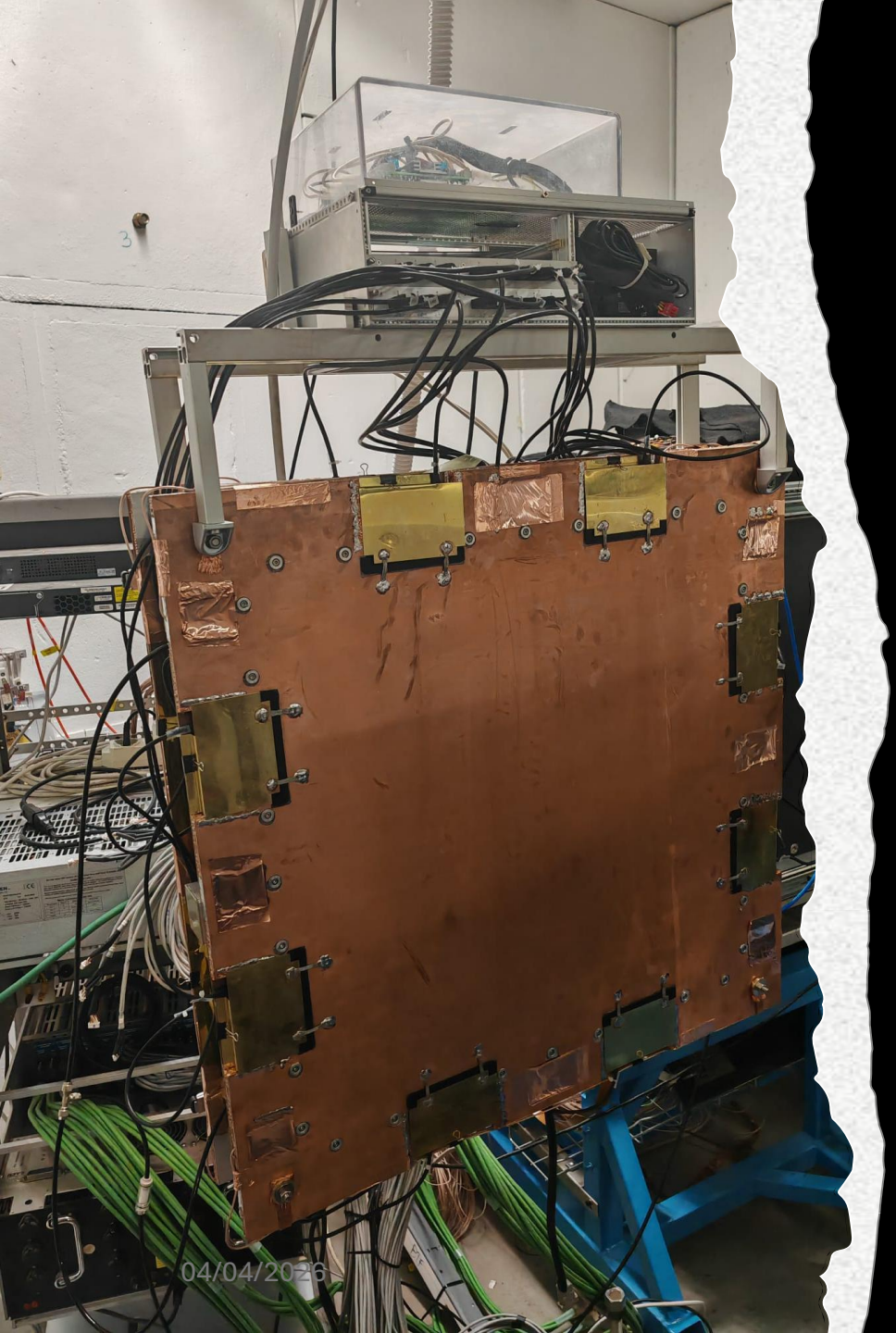

Il nuovo tracciatore MICROMEGAS di PADME

IFAE 2026 – Bologna

William Natale

Università Tor Vergata,

INFN – Laboratori Nazionali di Frascati

Positron Annihilation to Dark Matter Experiment

The Positron Annihilation to Dark Matter Experiment (**PADME**) is in the Beam Test Facility (**BTF**) at the Laboratori Nazionali di Frascati (**LNF**).

Born as a **missing mass experiment** searching for the Dark Photon A', using a e^+ beam (E<550 MeV) on a diamond active target.

Since 2022, PADME is devoted to **the search for X17 boson** through resonant production (first physics run called Run III).

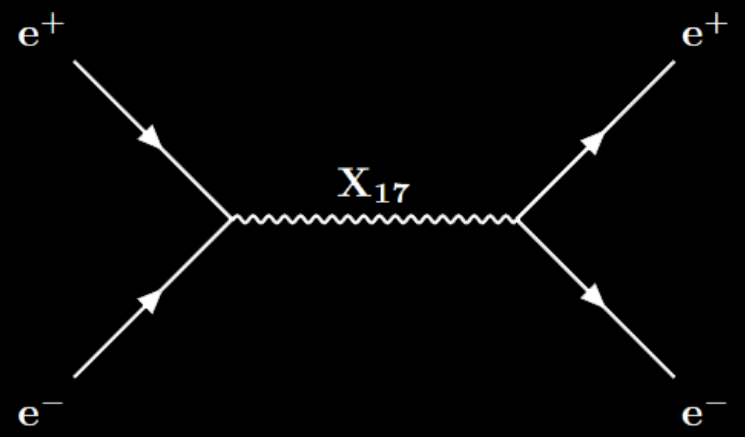

PADME X17 search: Run III result

Run III features:

- Expected width much smaller than centre of mass energy spread ~100 keV (1%$\sqrt{s}$ spread)
  → $\sqrt{s}$ scan in steps of 30 keV , between [16.4 MeV – 17.4 MeV] ← → [262 MeV – 296 MeV] beam energy

- Comparison of signal hypothesis vs SM background:

$$N_{2cl}(\sqrt{s}) = [\, B(\sqrt{s}) + S(\sqrt{s}) \,]$$
vs
$$N_{2cl}(\sqrt{s}) = B(\sqrt{s})$$

→ Found excess around **17 MeV/c^2**
corresponding to local 2.5σ
(global 1.8σ one-sided)

- 1% $\sqrt{s}$ spread = 0.3% $\oplus$ 0.9%
  Beam energy spread + electron motion

- Vector boson hypothesis for the test hypothesis plot

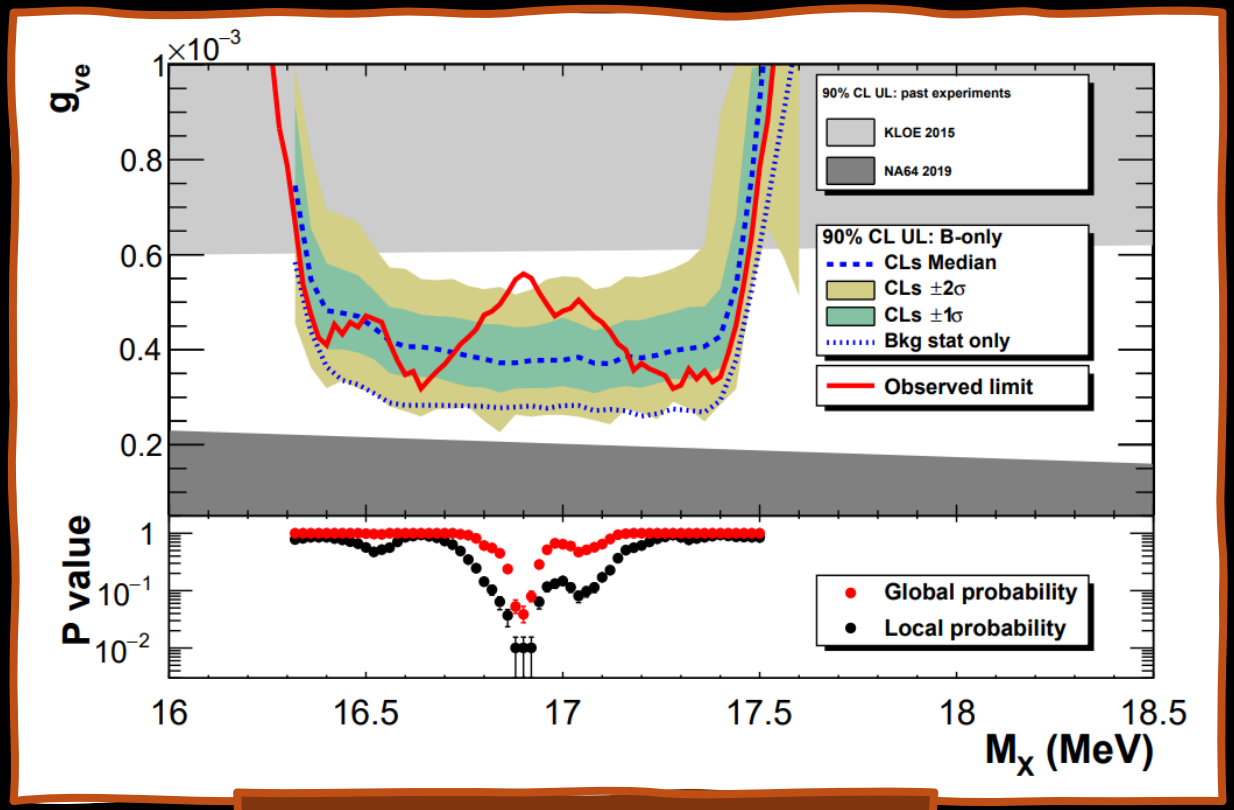

DOI: 10.1007/JHEP11(2025)007

Upgrade with MICROMEGAS detectors

Run III:

- Flux measurement & Beam related uncertainties
- Insufficient discrimination between charged/neutral particles from ETag
- Passive material of TimePix

Run IV upgrades:

- **Gaseous tracking detectors (padMMe and TMM)**
  - → **Discrimination of photons/charged particles**
  - → **Beam monitor capabilities**
- **Improved spatial and angular resolution**
- N_{ee} normalization to **another physical process**, like $N_{\gamma\gamma}$
- Reduced passive material along the beamline

Run IV: started June and ended in November

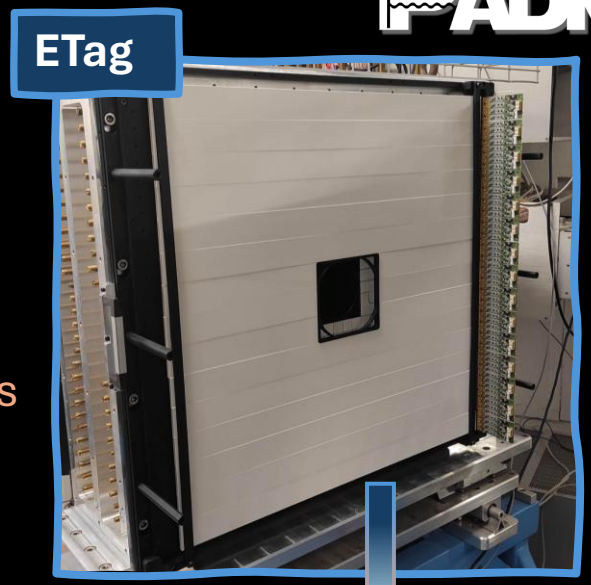

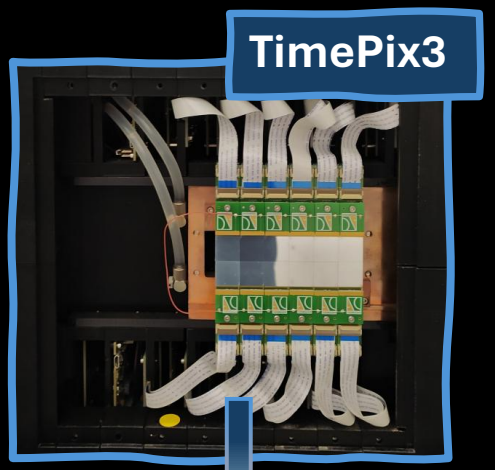

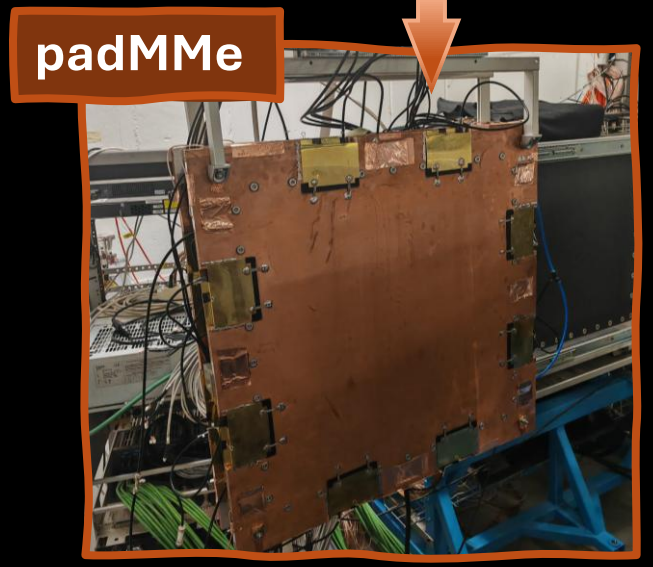

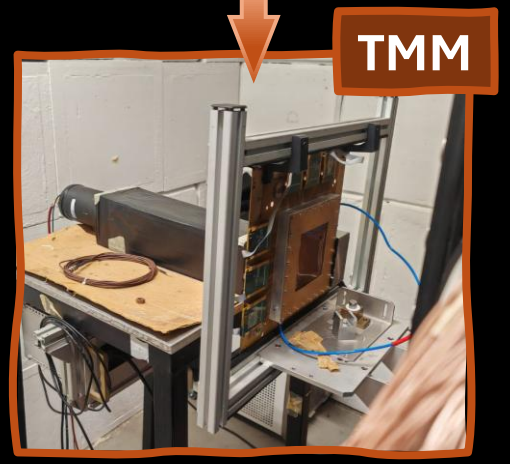

Gas detectors: MICROMEGAS

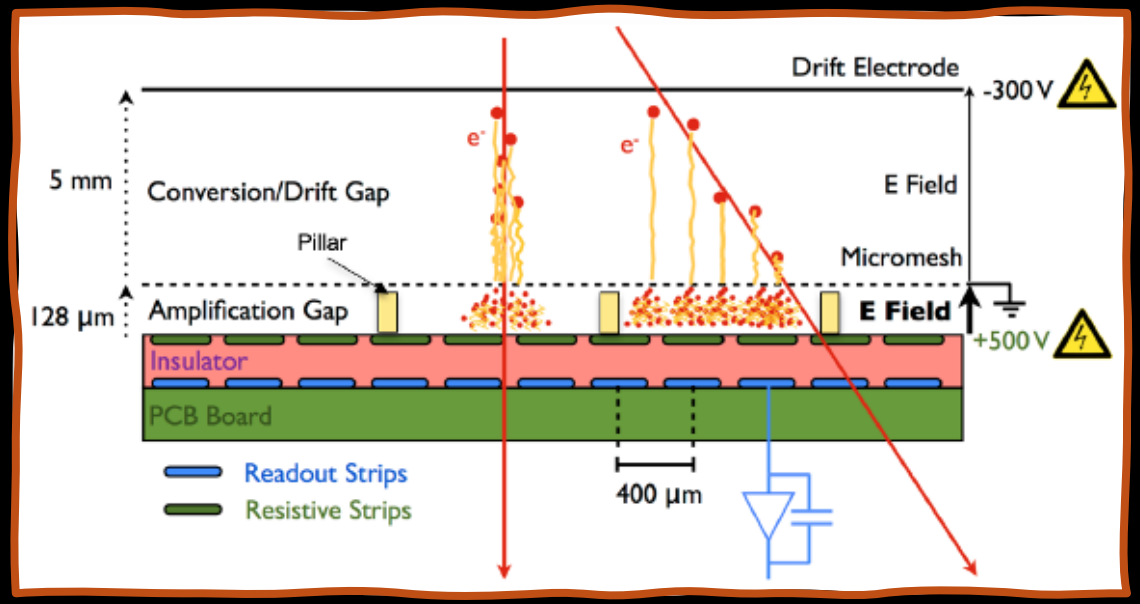

The **Micro-mesh-gas detectors** are a kind of **micro-pattern gas detector:**

- Drift gap (~mm/cm)
- Stainless steel mesh
- Amplification gap (~100 μm)

- **High amplification** ($\sim 10^4$) is achieved operating **close to spark limit** (Paschen)
  - → particular care of geometric tolerances
  - → **quenching by resistive layer + proper gas mixture**

- Readout by strips or pads
  - → signal by capacitive coupling with resistive layer.

The mesh could be bulk (fixed to readout PCB) or floating (fixed on a removable frame).

The usual ratio between the two electric fields is ~100 to make the **mesh transparent** to the electron entering the amplification gap.

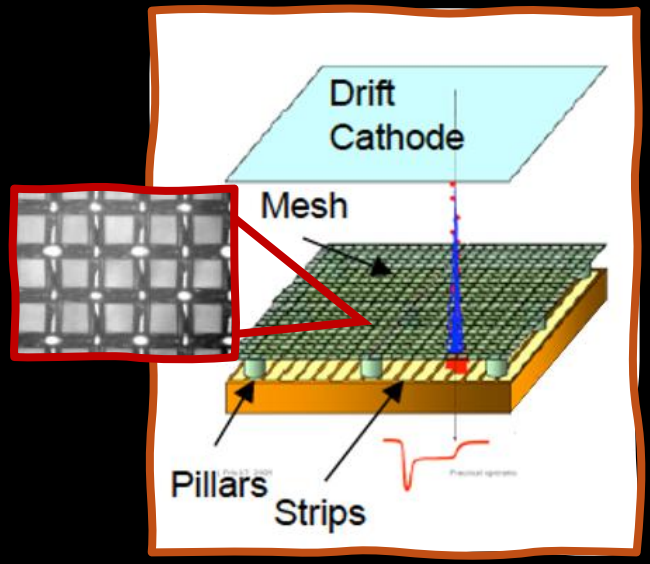

PADME MICROMEGAS detector: padMMe

The **padMMe** detector is a **floating mesh resistive anode Micromegas detector**, placed in front of ECAL.

The **active area is 65x65 cm^2**, with **two drift gaps of 5 cm** and two amplification gaps of 128 μm, each with a dedicated readout plane with **strips on both coordinates**.

The readout panel is made of FR4 - Honeycomb Nomex - FR4 sandwich glued to the PCBs.

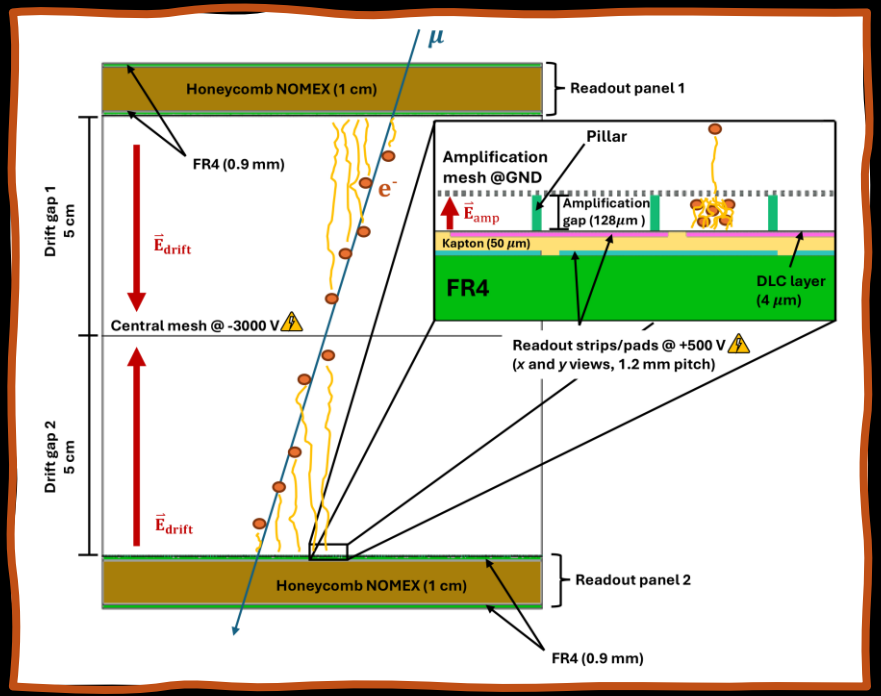

The mesh has stainless steel wires (18 μm of diameter, grid pitch of 45μm)

The gas mixture is **Ar**: CF_4: iC_4H_{10} = **88:10:2**
→ drift velocity = 10.5 cm/μs
→ ~100 total ionizations/cm

padMMe: readout features

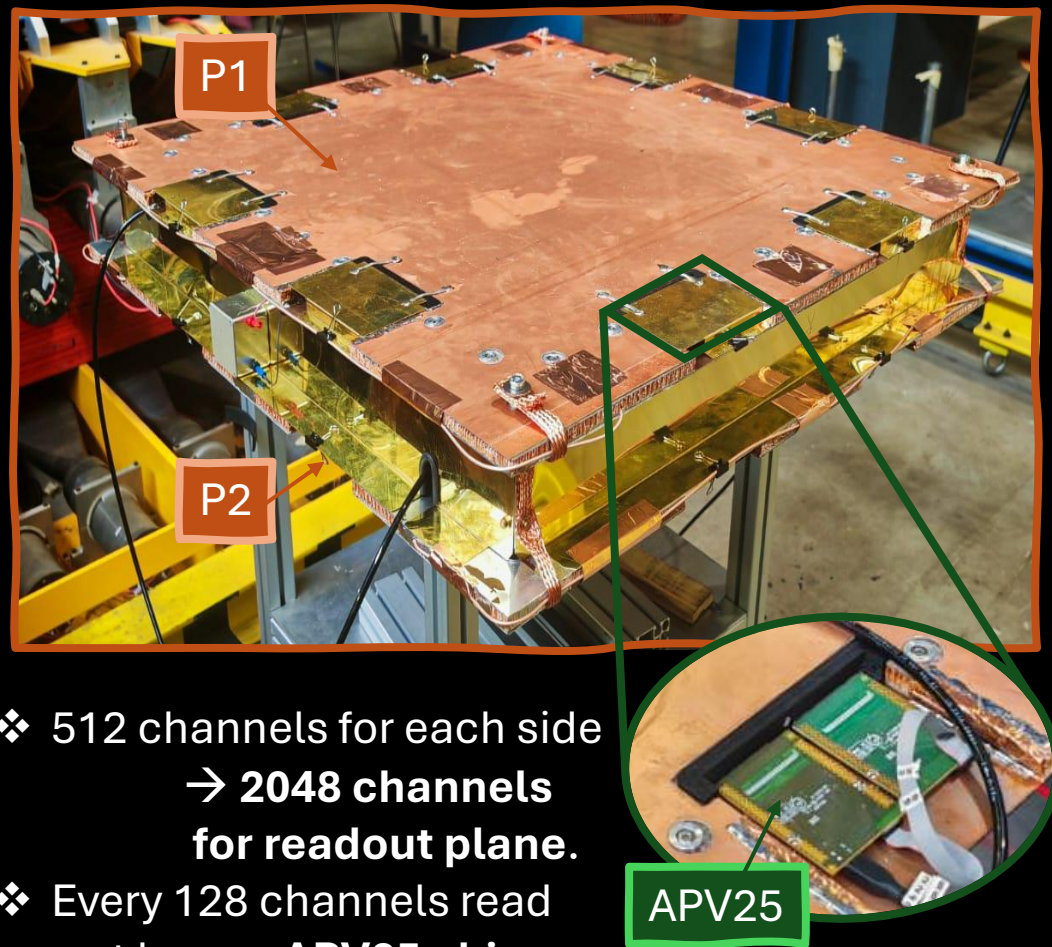

- 512 channels for each side → **2048 channels for readout plane**.
- Every 128 channels read out by one **APV25 chip**
- Each APV25 is connected to the Front-End Card for event building.

Two different segmentation layout tested:

- **straight strips**
- **rhomboidal strips**

→Same **pitch of 1.2 mm** (X, Y readout) → $\sigma_{X,Y} \sim$ **300** μm

→Expected Z-resolution **~ 1-2** mm.

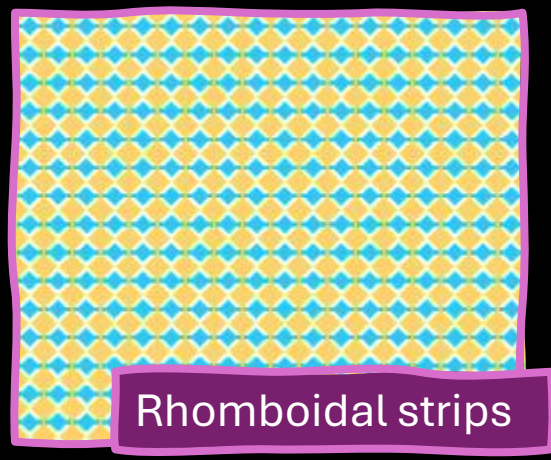

Rhomboidal strips now in PADME

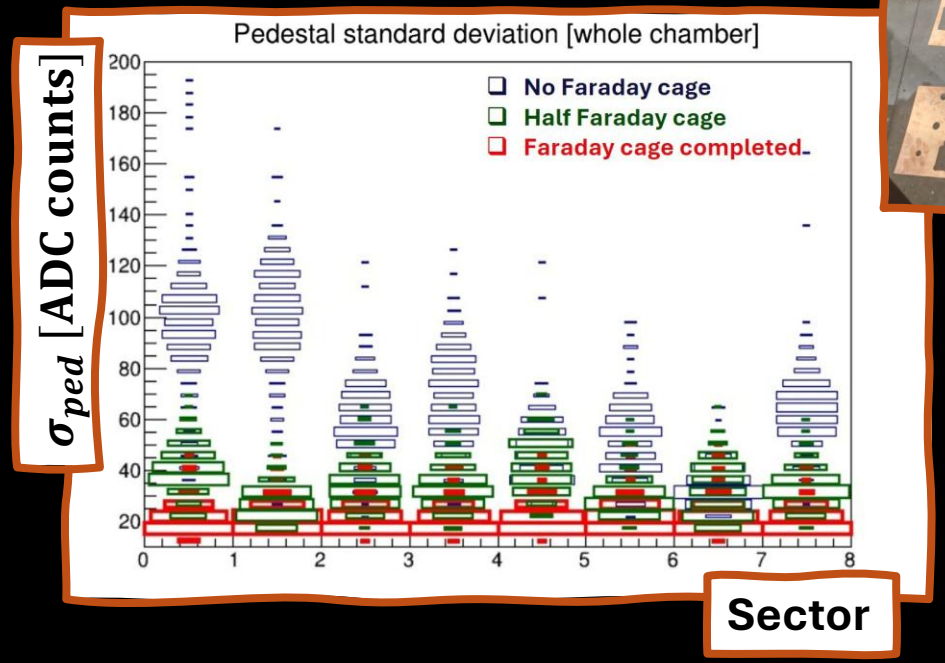

We improved the grounding and shielding of the chamber building a Faraday cage → **Electronic noise largely suppressed**

padMMe: HV features

The readout panel is made of two separate PCB glued together (producing a hole 7.2 mm). Moreover, the strip segmentation is adapted to have 4 quadrants for the whole panel.

The PCBs have **separate HV regions**, to enable operation in the beam region:

- An **inner circle** (R ~ 6 cm) → **low gain**
- A **middle ring** (ΔR ~ 4 cm) → **low gain**
- An **external zone** → **gain** ~ 10^4

The drift voltage is -3000 V
The nominal readout voltage:

- Inner circle → 350 V
- Middle ring → 350 V
- External zone → 490 V

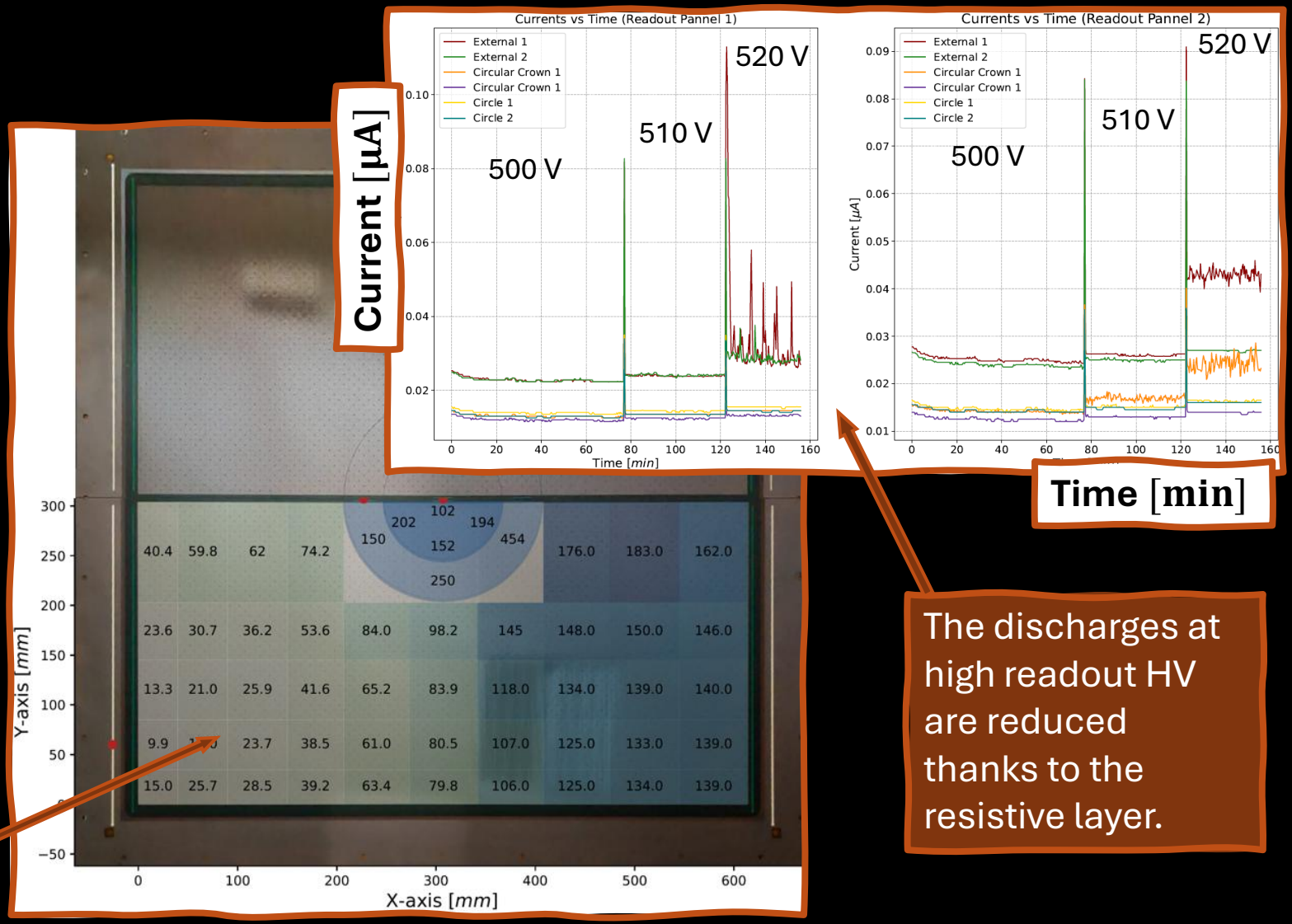

padMMe: Front End & DAQ

- APV25s are integrated in the Scalable Readout System which includes Front-End Cards.
- APV25 has a 200 ns charge integrator and 50 ns CR-RC shaper. Analog signal sampled at 40 MHz (25 ns).

- The padMMe DAQ window is 675 ns.
- The DAQ software is mmDAQ3
  → includes online monitor feature

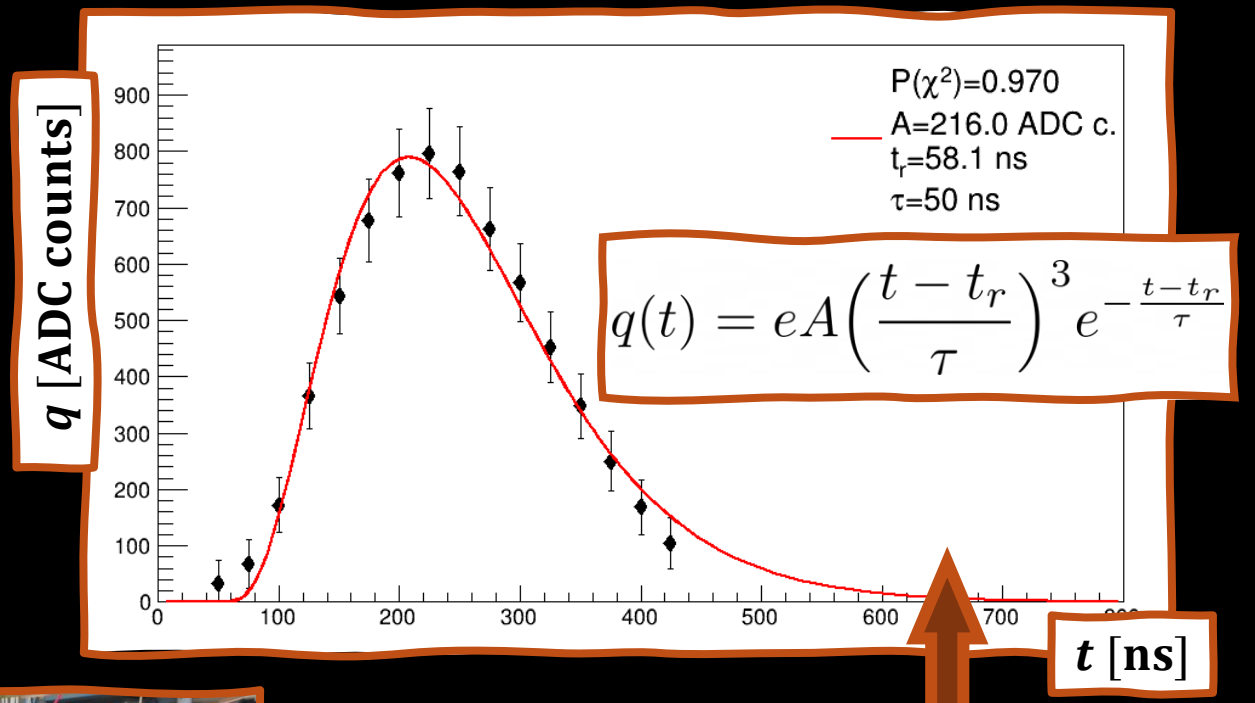

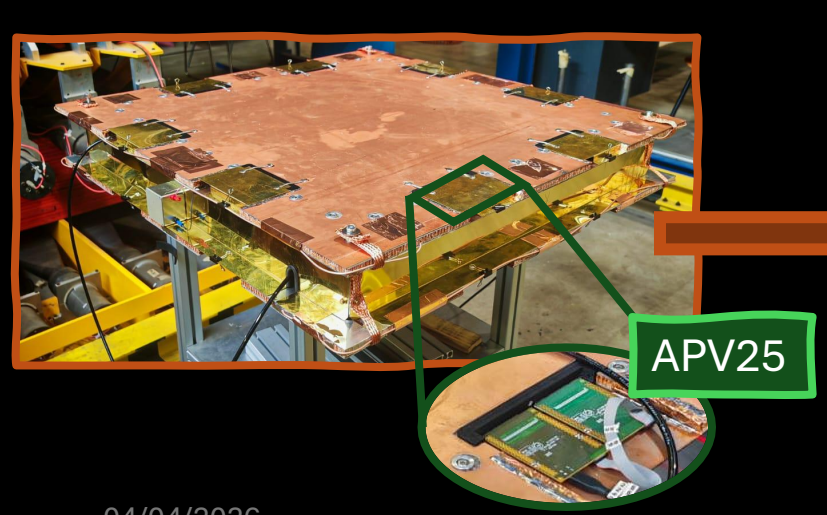

padMMe @ Cosmic Rays Stand

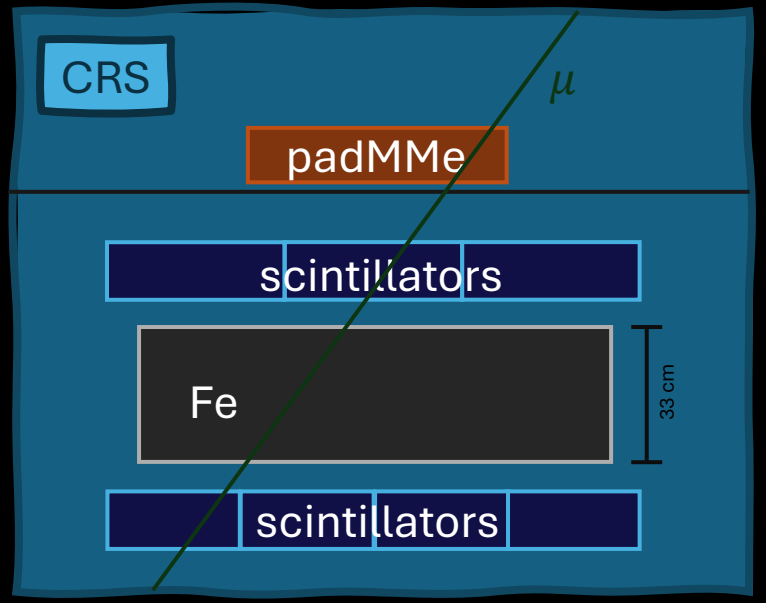

The padMMe was first tested and validated at the **Cosmic Rays Stand at LNF**, using cosmic rays, triggering with two sets of scintillators.

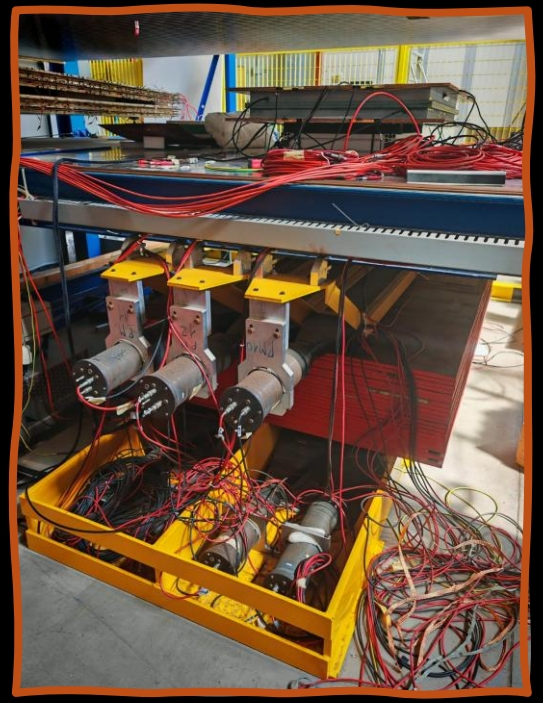

- Study **padMMe response vs readout HV**, to determine the HV work point:
  - measure of the **first Townsend coefficient α** → determination of **gain**
  - **hit efficiencies, ε_{hit}**

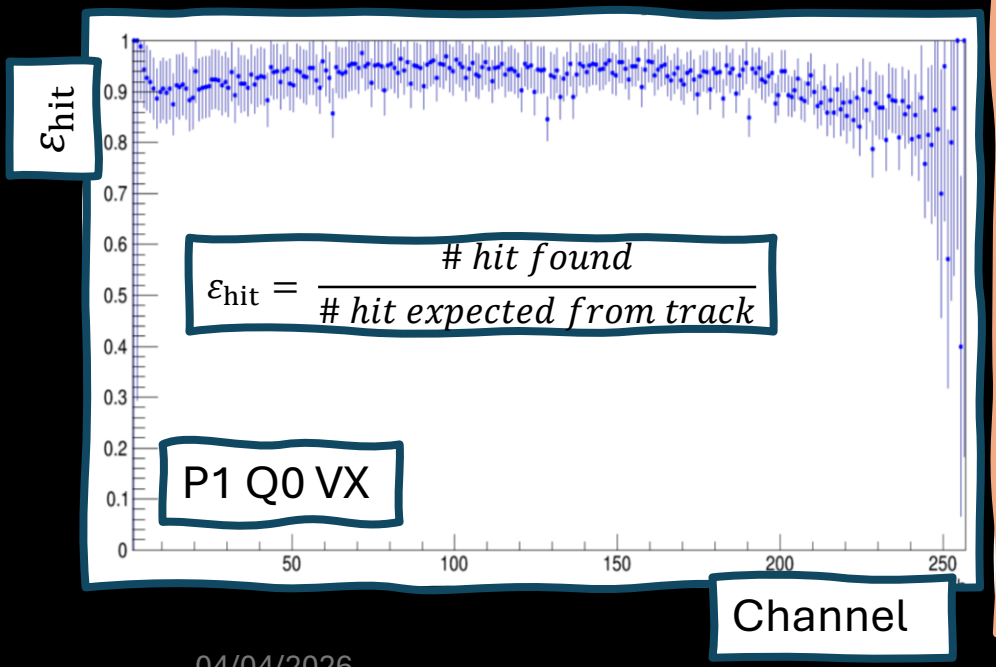

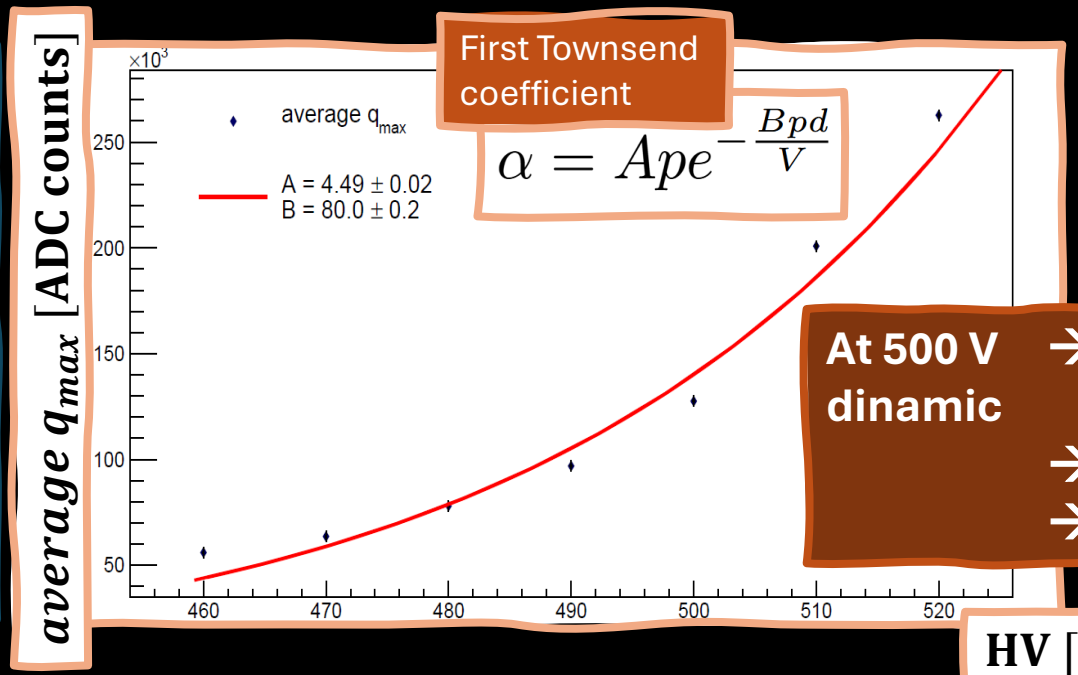

Pressure:
$p \sim 1\ bar * \sim 750\ mmHg$
Amplification gap:
$d = 128\ \mu m$
Applied voltage: V

At 500 V dinamic
→ **within ADC range**
→ **Gain** $= e^{\alpha d} \sim 10^4$
→ $\varepsilon_{hit} \sim 90\%$

* 4 mbar overpressure

padMMe @ CRS: reconstruction

We developed a reconstruction algorithm:

1. **Find the coordinates of the hits** → X and Y from strip position; Z from drift time: $Z = v_{\text{drift}}(t - t_0)$
2. **Clustering the hits in track candidates** (in average 1-2 candidates with 5-6 hits, per view)
3. **Fitting each candidate to find the track parameters** → $X = mZ + c$
4. **Matching top and bottom planes and x-y views**

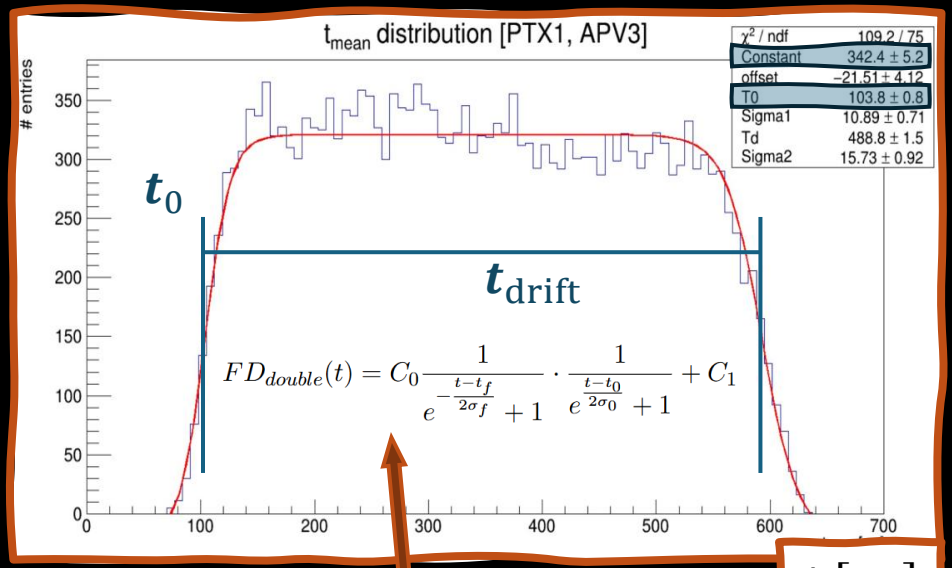

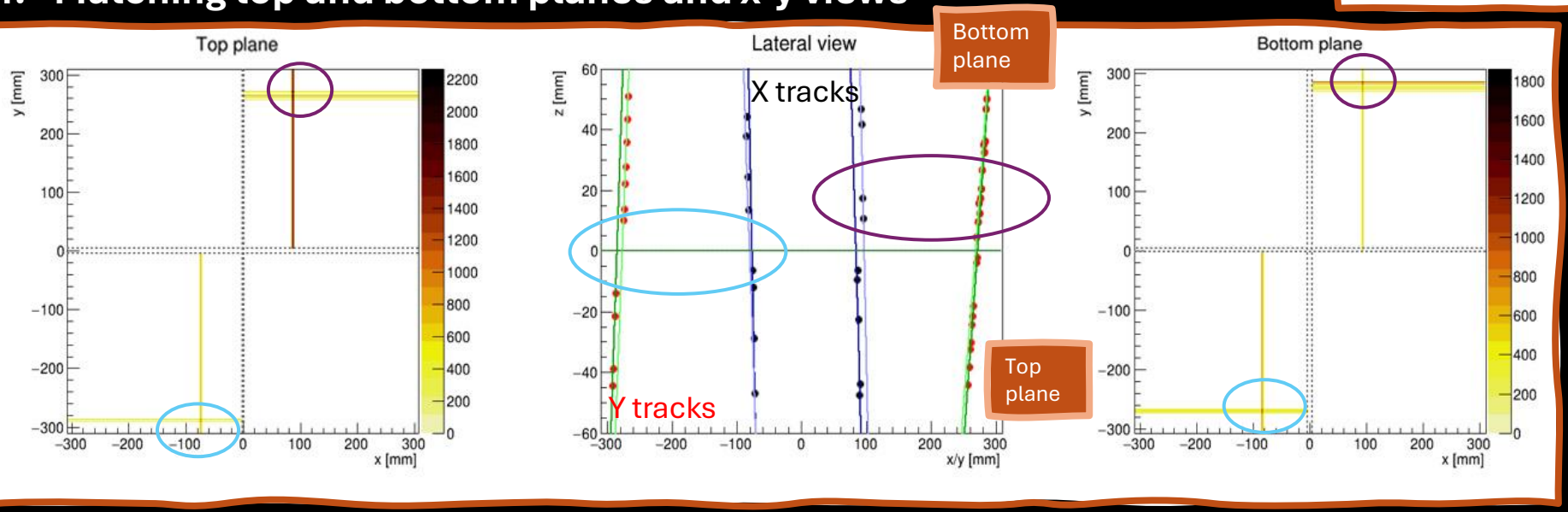

From the hit time distribution, we measured the drift velocity:

$$v_{\text{drift}} = d/t_{\text{drift}}$$

$$v_{\text{drift}} = 10.02 \pm 0.02 \text{ cm}/\mu\text{s}$$

padMMe @ CRS: resolutions

From the residues of the track reconstruction we were able to estimate the resolutions:

→ $\sigma_{x/y} \simeq 100\ \mu m$

→ $\sigma_z \simeq 700\ mm$ **(and constant with charge!)**

→ $\sigma_\theta \simeq 15\ mrad + 0.2\ |\theta|$

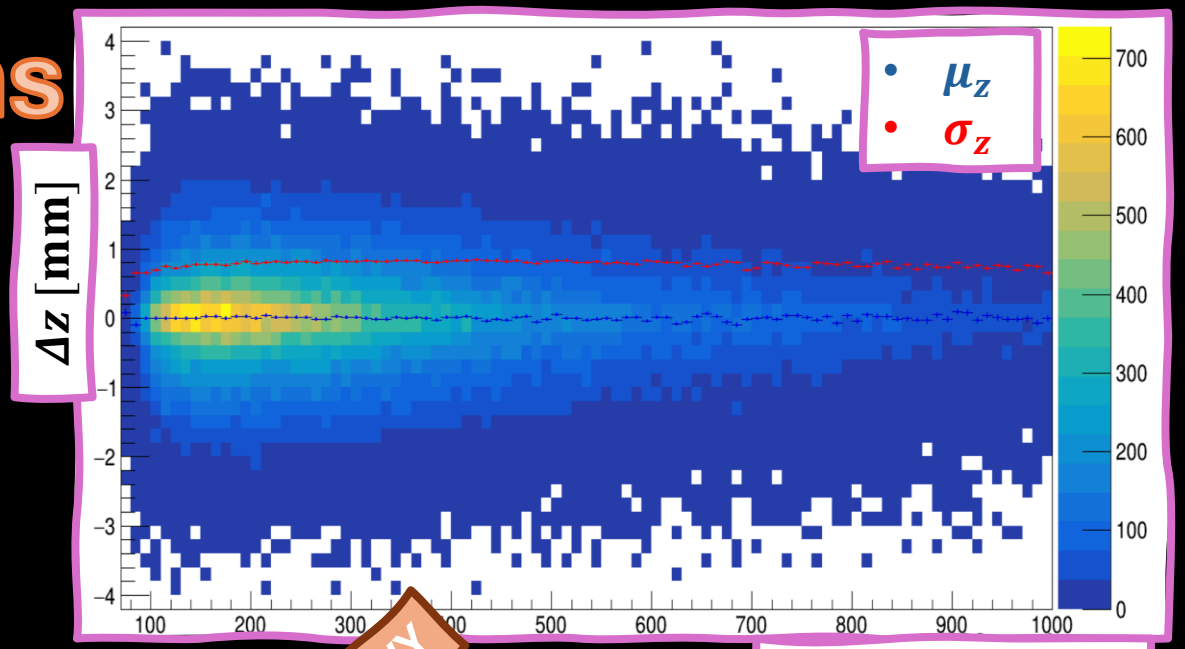

P2 Q3 VY

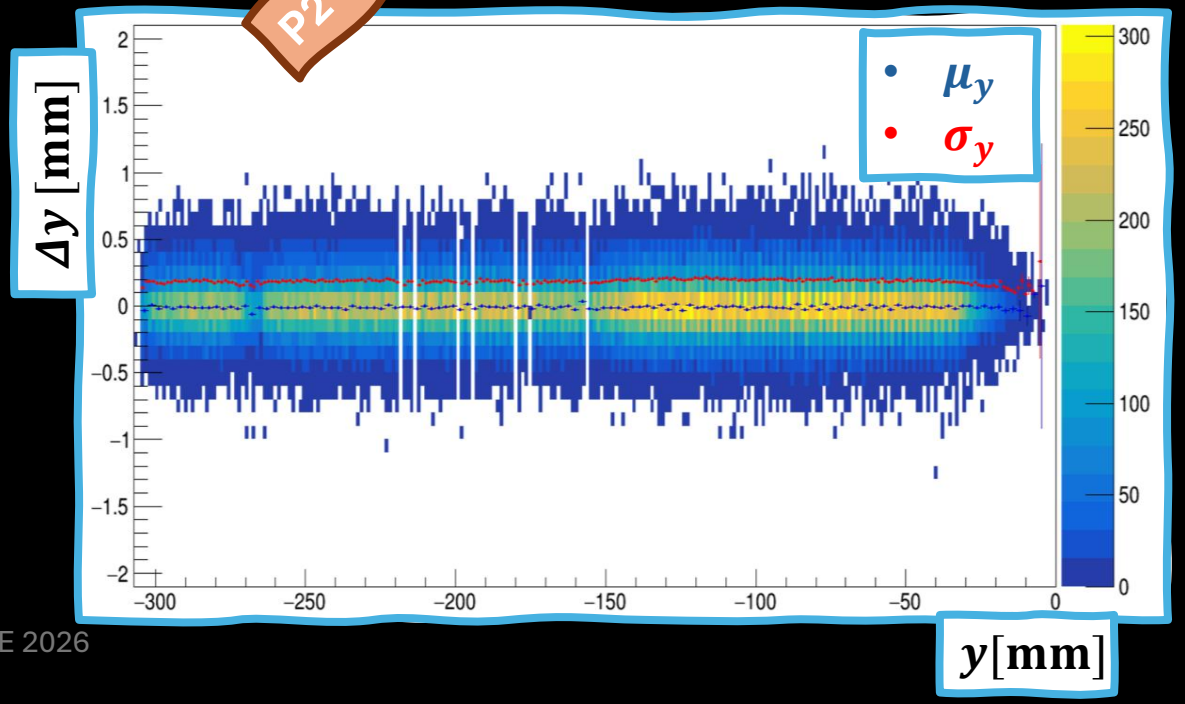

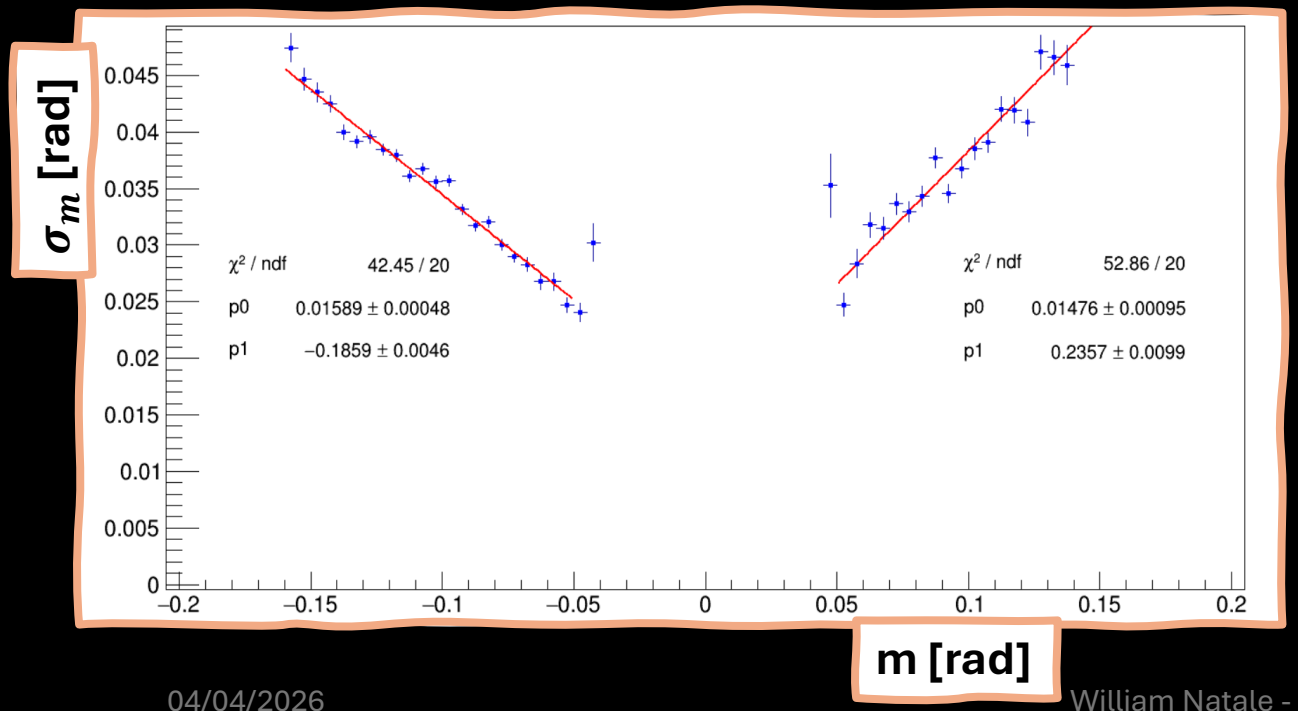

padMMe @ BTF: alignment

padMMe is jointly liable with ECAL, with a movable arm on the X axis.

We aligned padMMe with the PADME global reference system using 6 different aims glued on the two panels measured with a laser tracker.

On CAD drawing side we referred the positions of the aims to the strips position using a microscope.

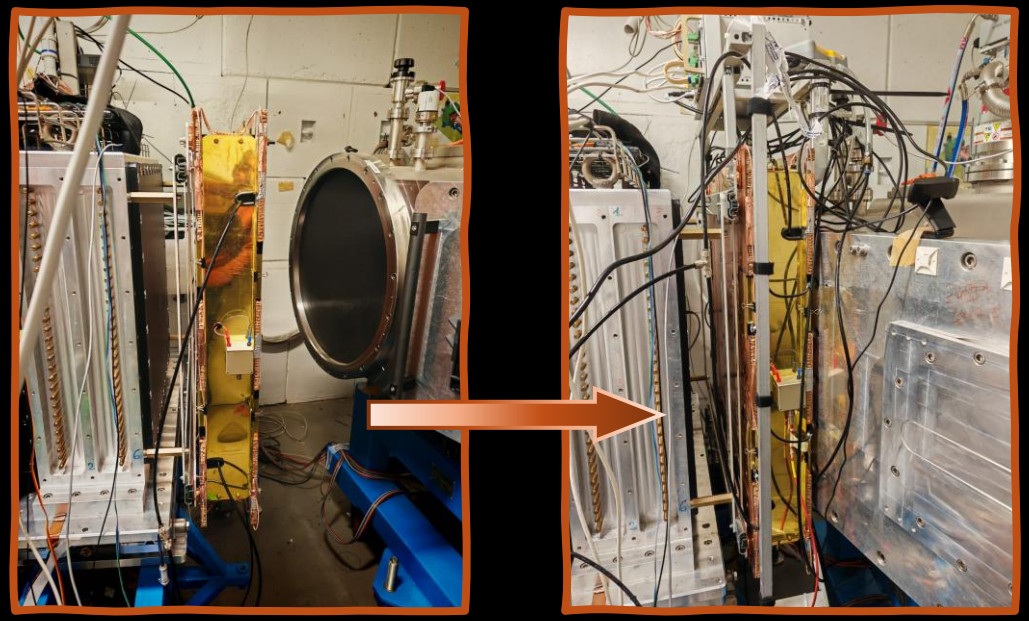

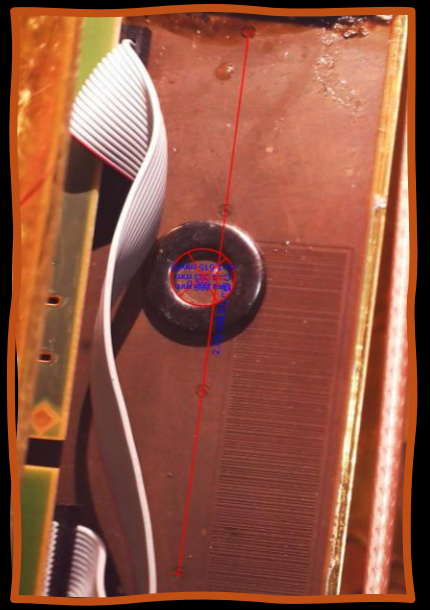

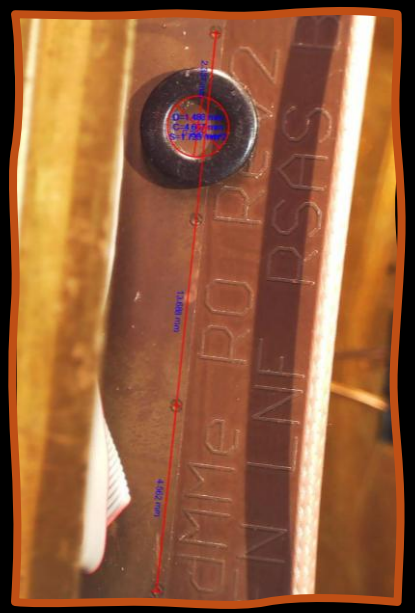

CAD crosschecked with redundant measurements
→ agreement within 300 μm

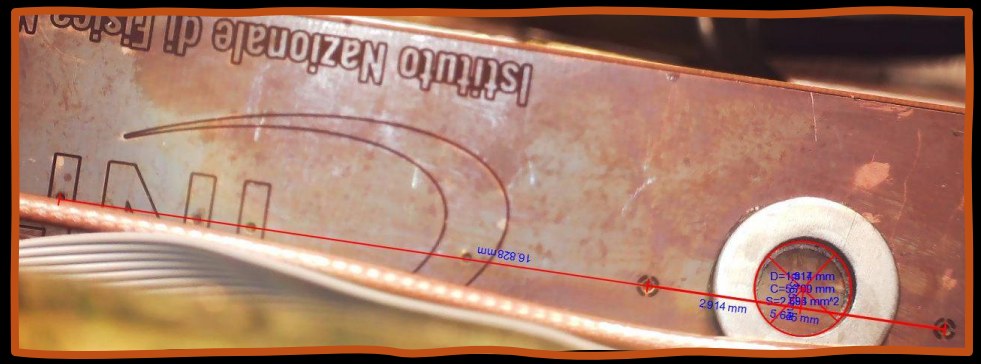

padMMe @ BTF: beam monitoring

Dedicated test runs to check beam monitoring:
- ❖ Inner circle → ionization chamber regime
- ❖ Middle ring → ionization chamber regime

padMMe slightly off-centred to avoid the dead area of the PCB junction.

Measured beam spread: $\sim 5.4 \times 5.4\ mm^2$

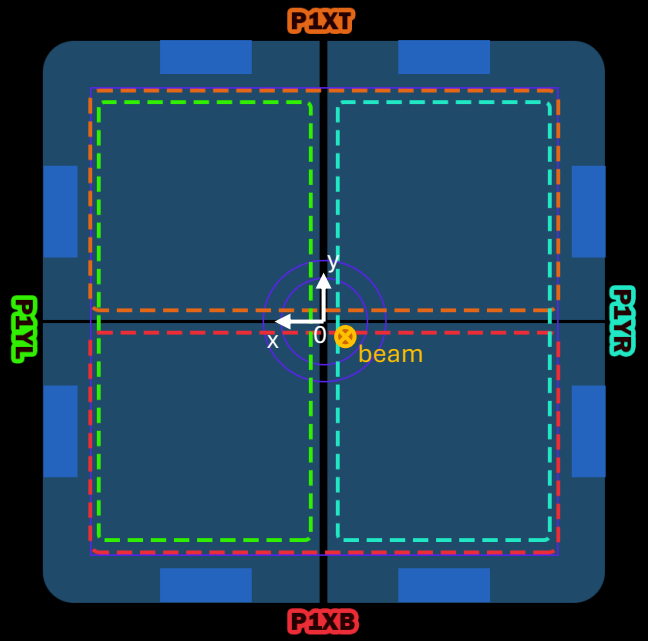

It's possible to evaluate beam position and spread with high precision using padMMe

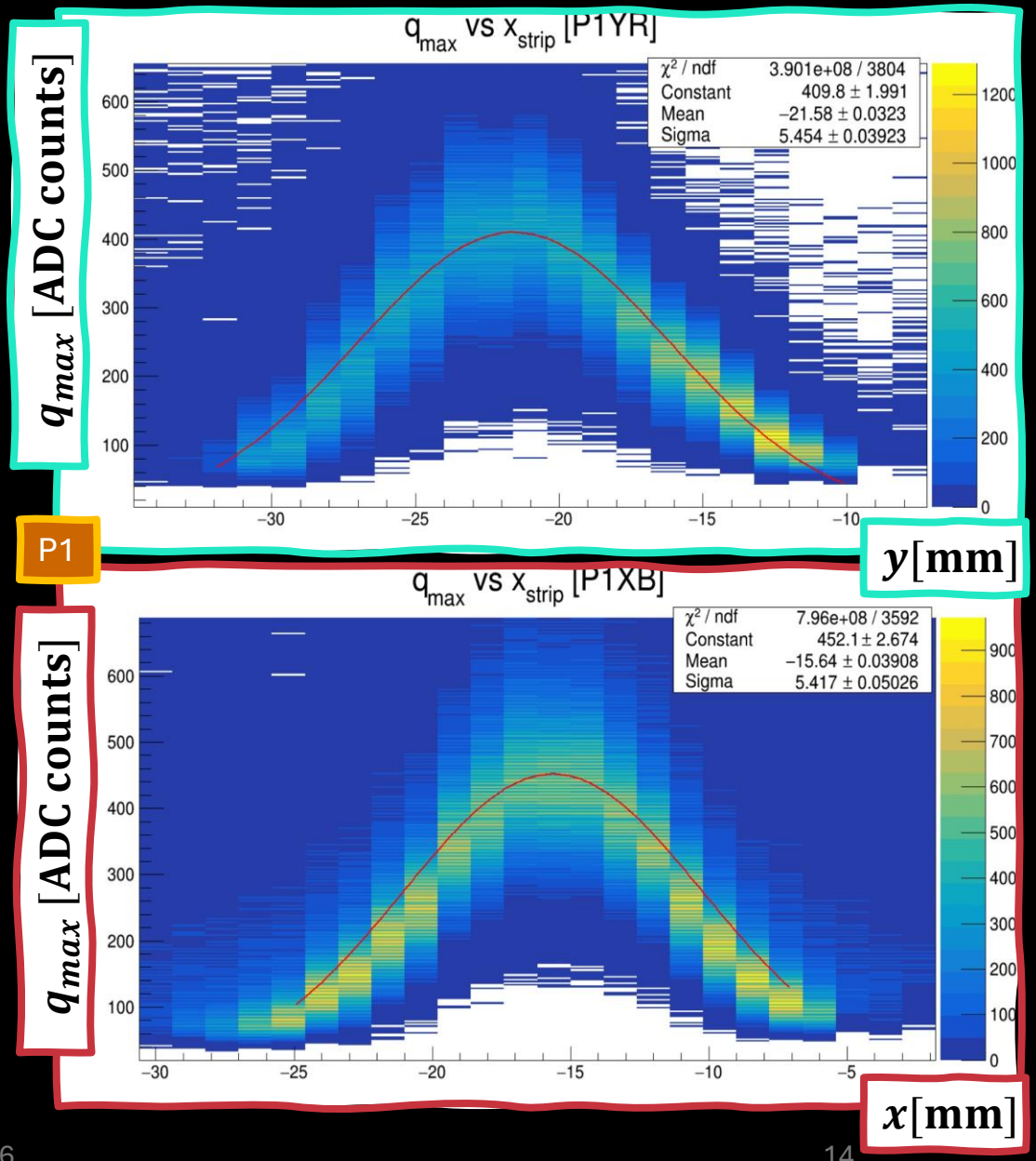

padMMe @ BTF: commissioning measurements

Having the **beam spread measurement at target and at padMMe** we were able to compute:

Target Multiple Coulomb Scattering

@ padMMe

$$\theta_{MCS}^{exp} = \frac{\sqrt{\sigma^2_{target-in} - \sigma^2_{target-out}}}{d_{target-padMMe}}$$

$$\theta_{\mathrm{MCS}}^{\mathrm{exp}} = 0.88 \pm 0.01 \ \mathrm{mrad}$$

Beam divergence θ_{div} and **normalized emittance** ε

$$\theta_{div} = \frac{\sqrt{\left(\sigma_x^{padMMe}\right)^2 - \left(\sigma_x^{target}\right)^2}}{d_{target-padMMe}}$$

$$\theta_{\mathrm{div}} = 1.08 \pm 0.07 \ \mathrm{mrad}$$

Target out!

$$\varepsilon_{RMS} = \theta_{div} \cdot \sigma_x^{target}$$

$$\varepsilon = \beta\gamma\varepsilon_{RMS}$$

$$\varepsilon = 0.8 \pm 0.2 \ \mathrm{mm\ mrad}$$

padMMe @ BTF: reconstruction

Huge combinatory in pattern recogniction

- ~ 3500/4096 fired strips → ~85% occupancy
- ~200 track candidates found w/o Interaction Point (IP) constraint

  → **IP oriented pattern recognition algorithm**

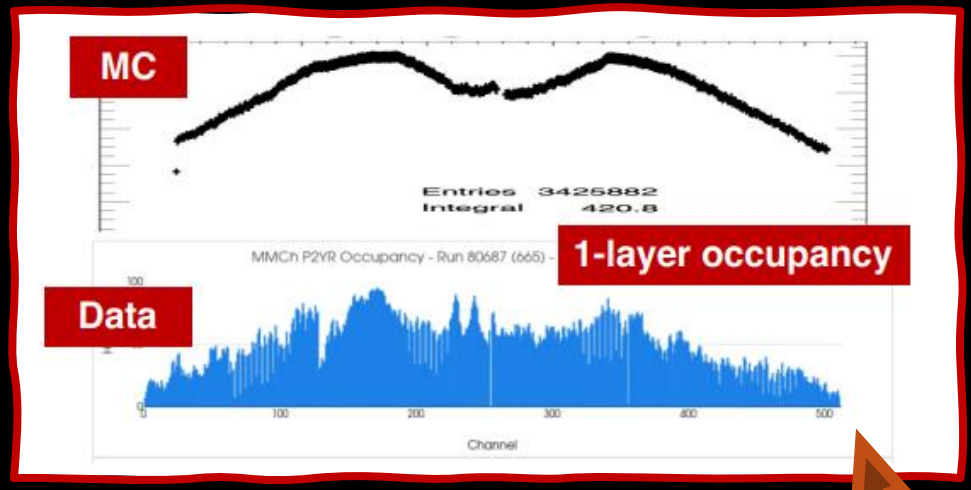

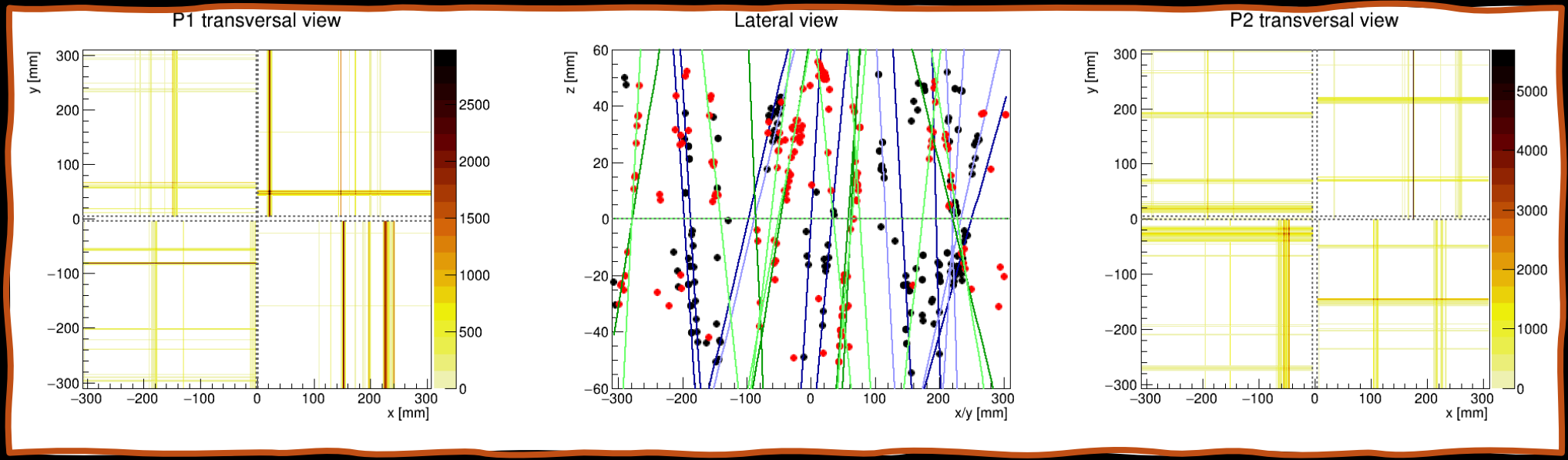

Data and MC simulation agree

padMMe @ BTF: reconstruction

For each charged particle we expect 4 tracks (2D) → **Level-0 tracks**

→ High efficiency but a Level-0 track requirement has high bkg component (combinatorial)

→ **need at least 2/3 out of 4 coincidences** two-planes coincidence → **Level-1 track** to be matched with Ecal clusters

Track-to-Ecal-Cluster association

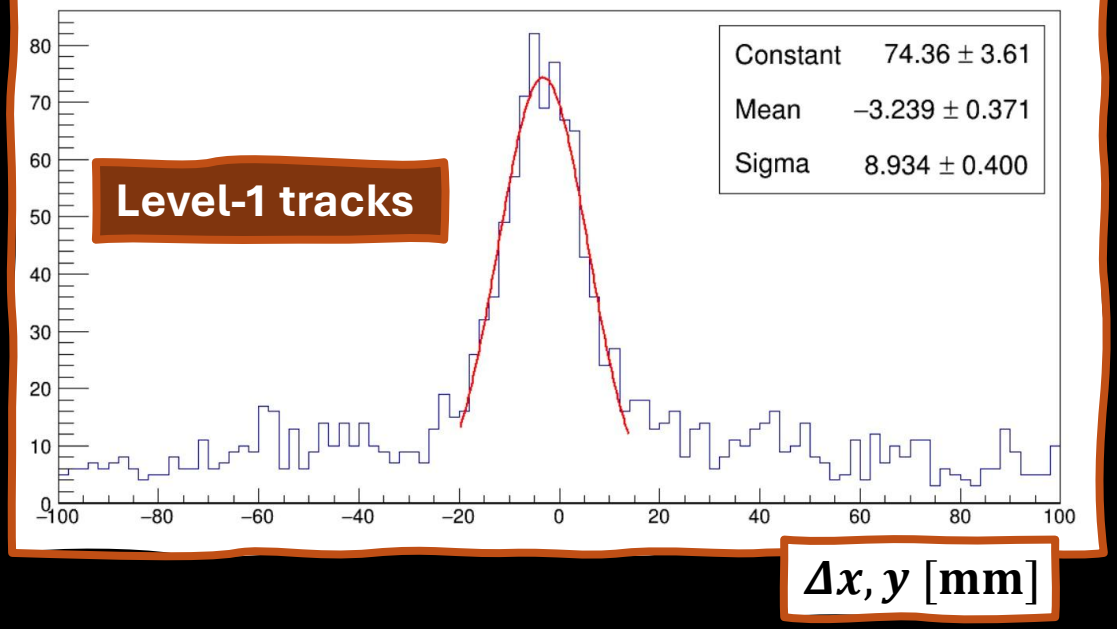

Track direction residuals

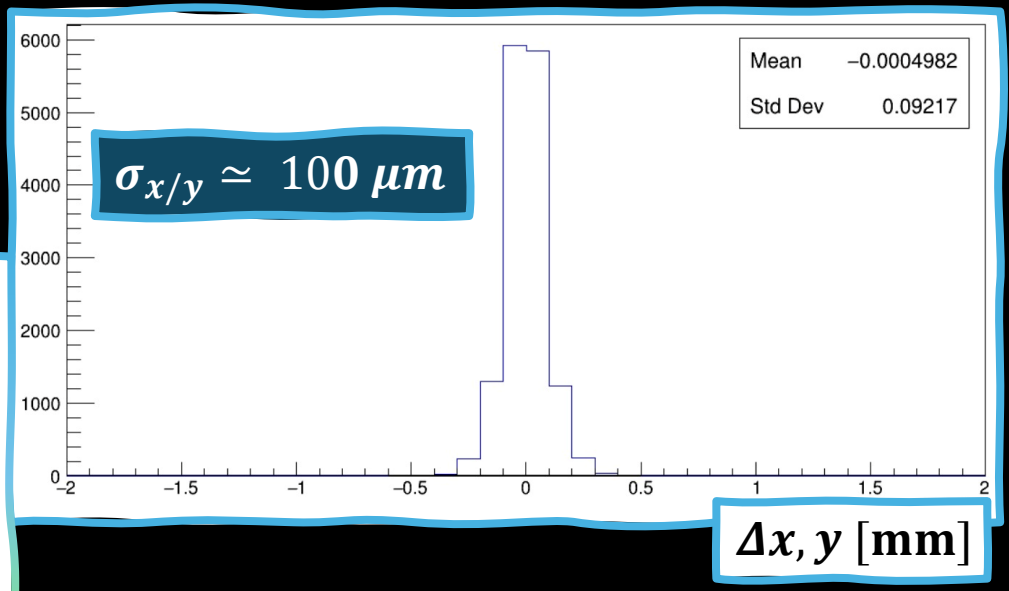

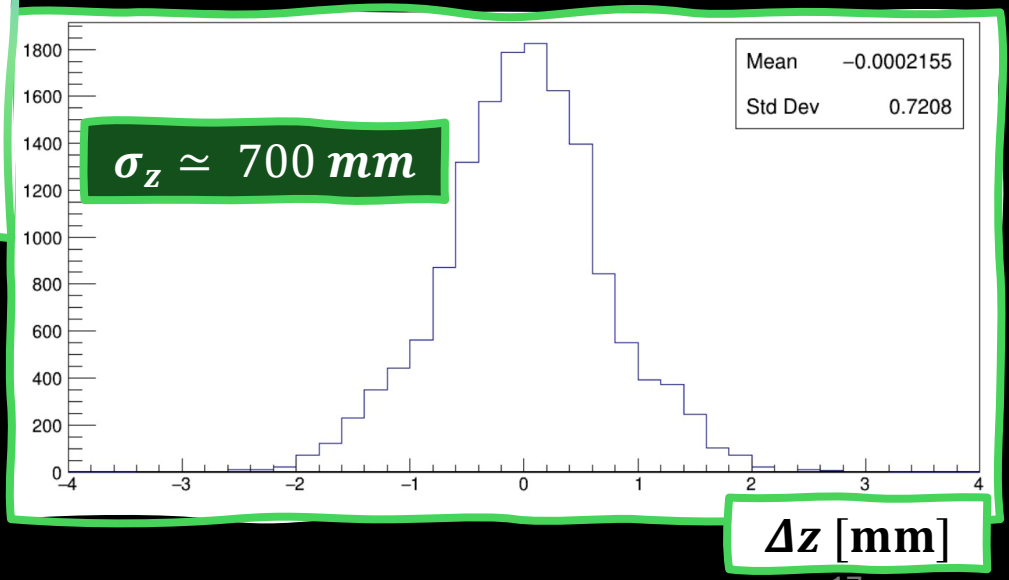

Summary and conclusions

PADME Run IV upgrade:

- **Building of a new Micromegas tracking detector** for the identification and reconstruction of charged particles:
  - → **Double floating mesh resistive anode panel with 2x5 cm drift gaps**
  - → **Double X and Y readout (4096 strips tot)**
    - → **Noise study and Faraday cage construction**
    - → **Quality tests**: deformation of the panels, gas tightness, HV study, dimensional measurements (pillars heigh, mesh tension)

- **Analysis of cosmic ray data:**
  - → **Gain Characterization** → **@ 500V: 90% hit efficiency + 10^4 gain**
  - → **Tracks reconstruction and performances**
    - → **found resolutions** (same for Run IV data)

$$\sigma_{x/y} \simeq 100\ \mu m$$
$$\sigma_z \simeq 700\ mm$$
$$\sigma_\theta \simeq 16\ mrad$$

- After **installation in the experimental apparatus** and **Alignment:**
  - → **Commissioning and beam parameters measurements** (position, spread, divergence, emittance and target MCS)

- **Official PADME data taking:** currently reconstructing data

Thanks for your attentions :)

Backup slides

The X17 anomaly

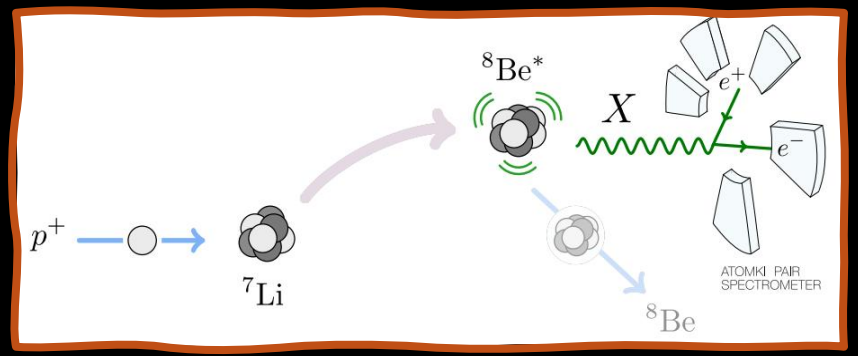

Excesses in angular distribution of e^+e^- pair in nuclear transitions of ^8Be, ^4He e ^{12}C observed by the **ATOMKI collaboration.**

This anomaly happens at **different angles for different energy transition.**

All of them are compatible with the hypothesis of the production and subsequent decay of a **new particle with mass ~17 MeV**.

MEG-II searched for this anomaly in the ^8Be **transitions** with a dedicated data taking, setting upper limits 90% C.L. on the branching fractions:

$$R_{17.6} < 1.8 \times 10^{-6} \quad , \quad R_{18.5} < 1.2 \times 10^{-5}$$

Don't exclude completely the region suggested by ATOMKI results.

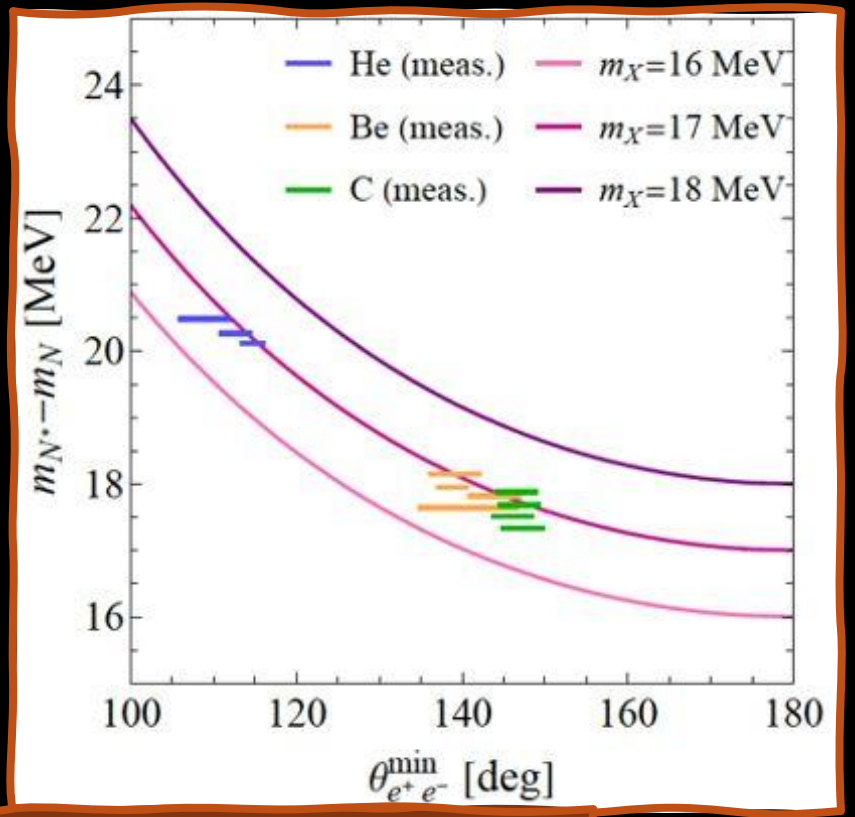

PHYS.REV. D 108, 015009 (2023)

X17 anomaly @ ATOMKI

18.5 MeV ^8Be transition

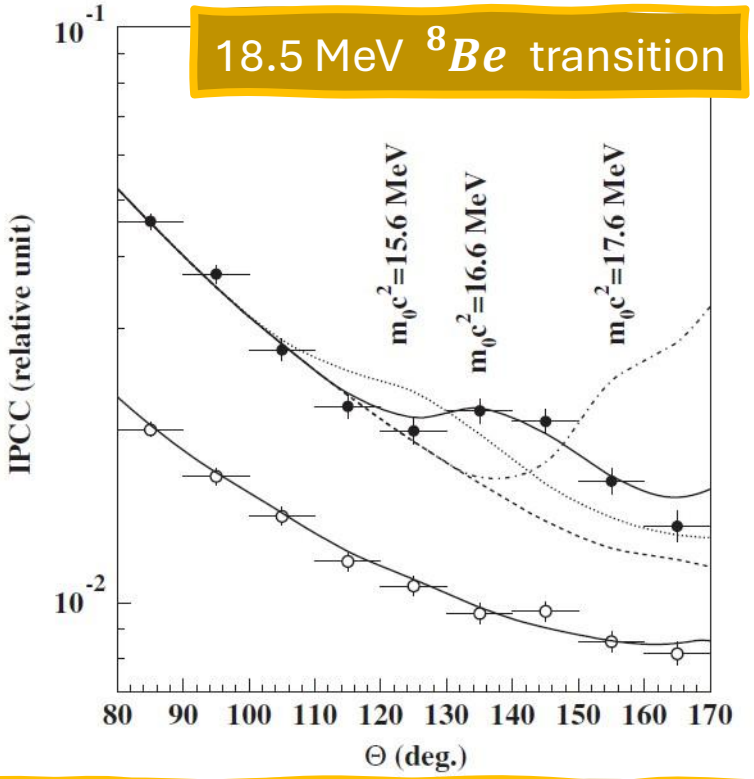

PhysRevLett.116.042501 (2016)

PhysRevC.104.044003 (2021)

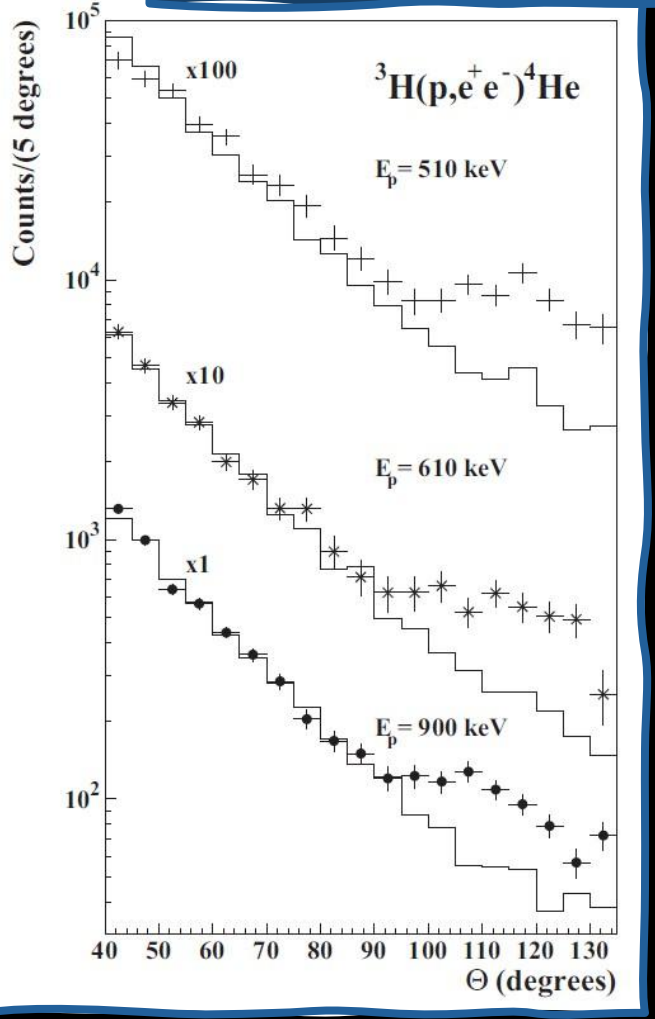

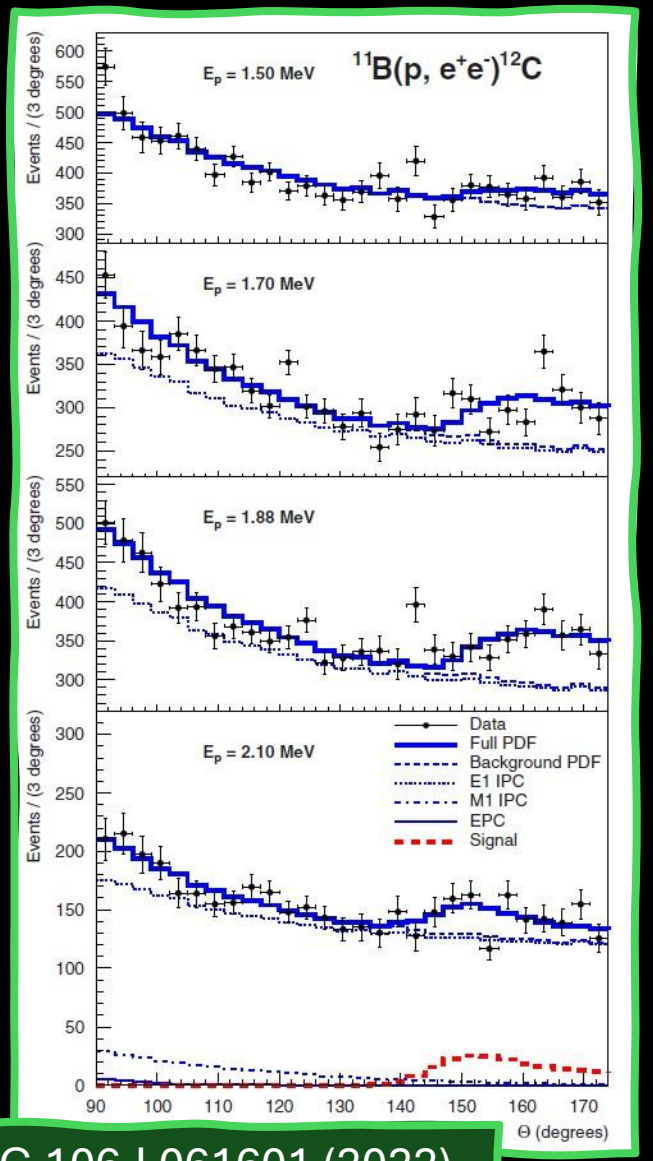

PhysRevC.106.L061601 (2022)

MEG-II VS ATOMKI

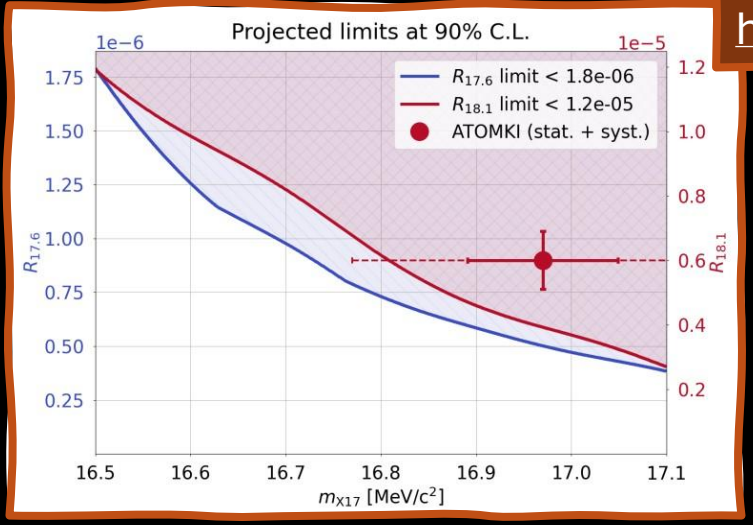

https://arxiv.org/abs/2411.07994

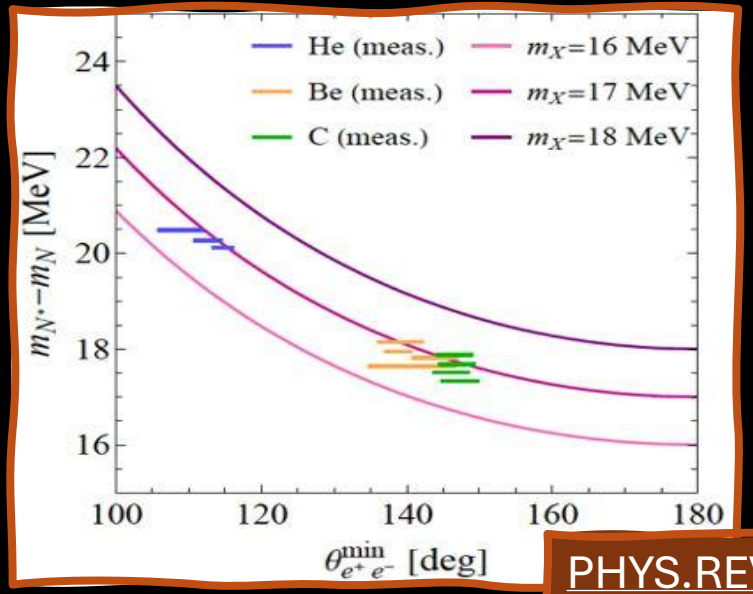

PHYS.REV. D 108, 015009 (2023)

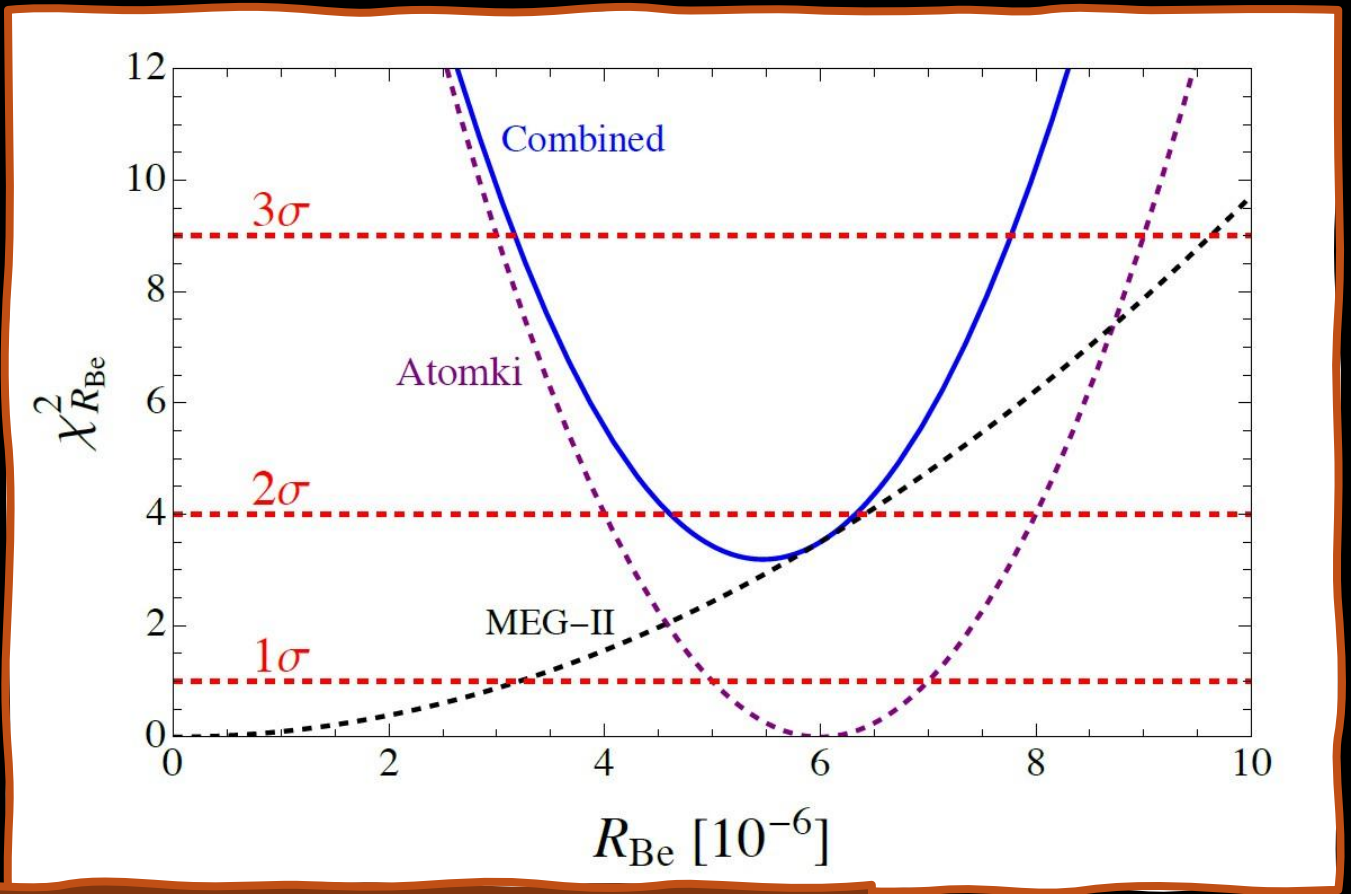

http://dx.doi.org/10.1007/JHEP04(2025)035

X17 boson nature

N^*	$J^{P_*}_*$	J^P (f.s.)	scalar X	pseudoscalar X	vector X	axial-vector X
^{8}Be (18.15)	1^+	0^+	...	✓	✓	✓
^{4}He (21.01)	0^-	0^+	...	✓	...	✓
^{4}He (20.21)	0^+	0^+	✓	...	✓	...
^{12}C (17.23)	1^-	0^+	✓	...	✓	✓
^{8}Be (GDR $\to g.s.$)	1^-	0^+	✓	...	✓	✓
^{8}Be (GDR $\to 2^+_1$)	1^-	2^+	✓	✓	✓	✓

X17 as a Vector boson

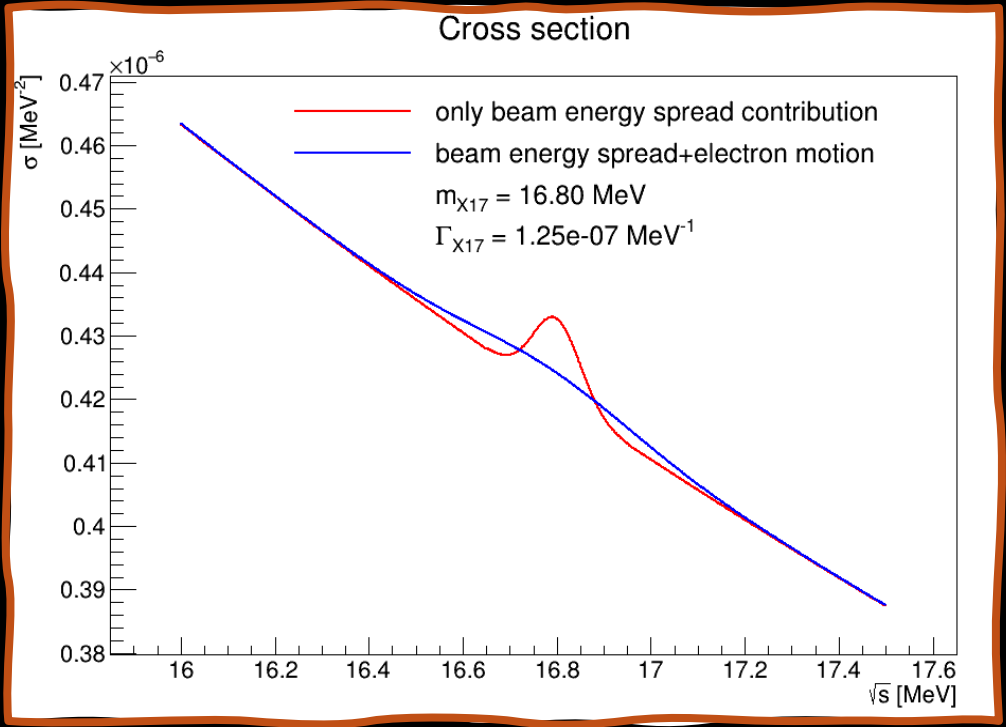

$$\frac{d\sigma}{d\cos\theta} = \frac{\alpha(s)^2}{4s}\frac{(3+cos^2\theta)^2}{(1-cos\theta)^2}$$ **T-channel**

$$+\frac{9\,s\,\Gamma_{X_{17}}(s)^2}{4\,m^2}\frac{(1+cos^2\theta)}{(s-m_{X_{17}}^2)^2+s\,\Gamma_{X_{17}}(s)^2}$$ **S-channel**

Interference term

$$+\left[(1+cos^2\theta)-\frac{(1+cos\theta)^2}{1-cos\theta}\right]\frac{3\,\alpha(s)\,\Gamma_{X_{17}}(s)}{2\,m}\frac{(s-m_{X_{17}}^2)}{(s-m_{X_{17}}^2)^2+s\,\Gamma_{X_{17}}(s)^2}$$

Run III: experimental setup

Active Target (diamond)

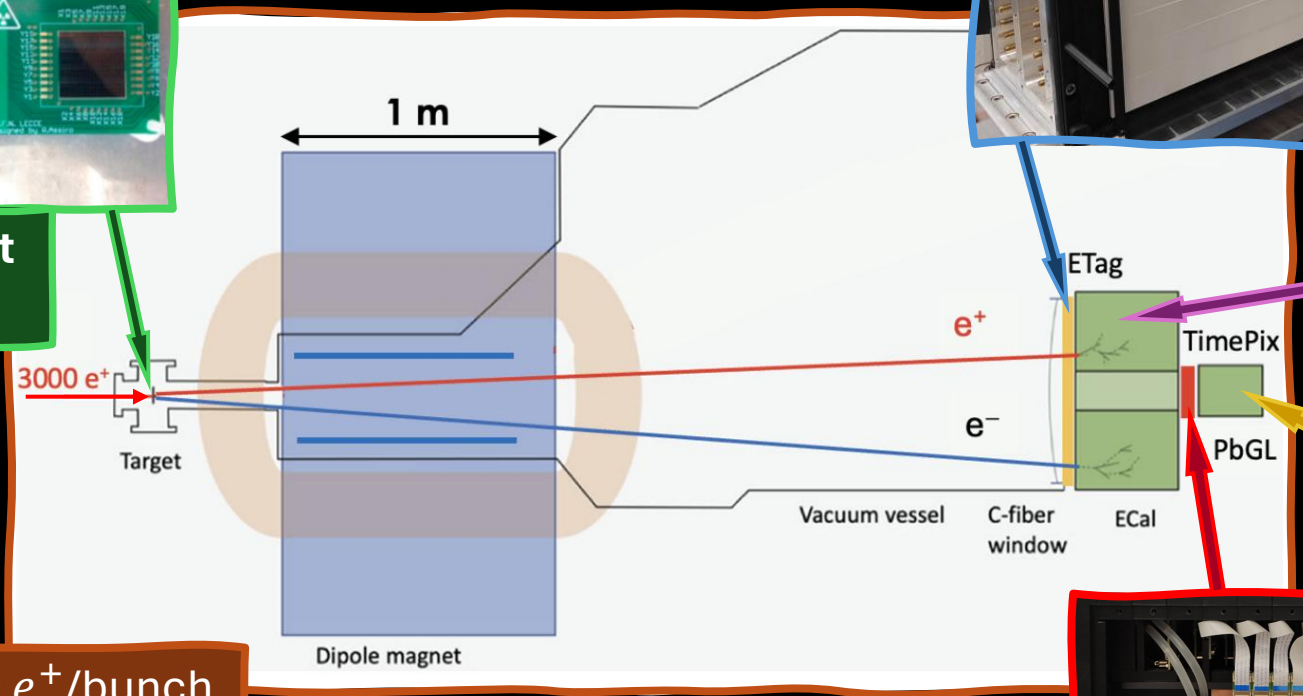

Beam: 3000 e^+/bunch
[262 MeV – 296 MeV]
Bunch length ~200 ns

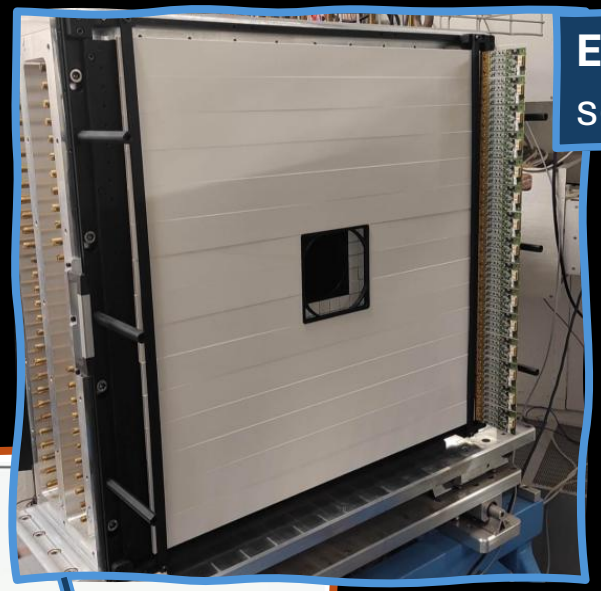

ETag (18 plastic scintillators 4x60x0.5 cm^3)

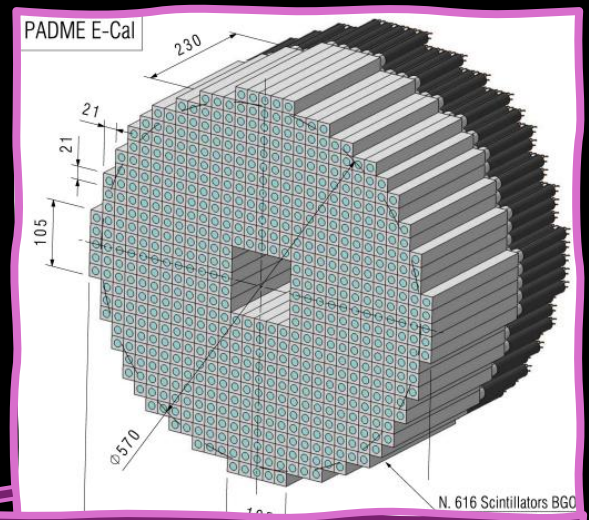

ECAL (616 BGO crystals 21×21×230 mm^3)

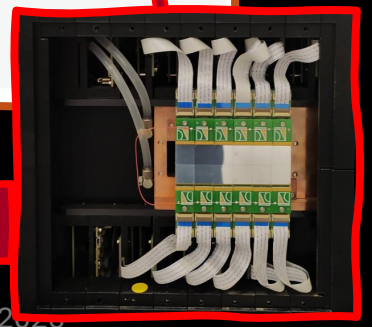

TimePix3

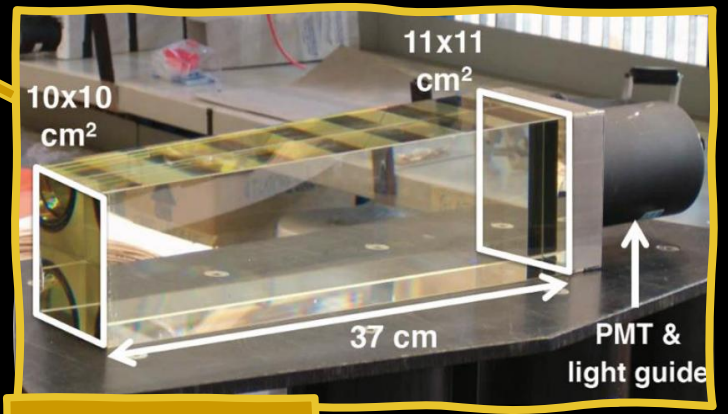

LeadGlass

Run III: analysis & results

Run III features:

- Intrinsic width ~ eV or smaller (from ATOMKI) while experimental width ~100 keV ($\sqrt{s}$ spread)
  → $\sqrt{s}$ scan in steps of 30 keV , between [16.4 MeV – 17.4 MeV] ← → [262 MeV – 296 MeV] beam energy

- Vector boson hypothesis → coupled to EM current

- Comparison of signal hypothesis vs SM background:

$$N_{2cl}(s) = N_{POT}(s) \times [\, B(s) + S(s; M_X, g)\, e_S(s) \,]$$

vs

$$N_{2cl}(s) = N_{POT}(s) \times B(s)$$

→ Found excess at $m_x c^2 = (16.90 \pm 0.02)$ **MeV**
$g_{ve} = 5.6 \times 10^{-4}$, $\Gamma_{exp} \sim 100$ keV
corresponding to local 2.5σ
global (1.77 ± 0.15) σ one-sided

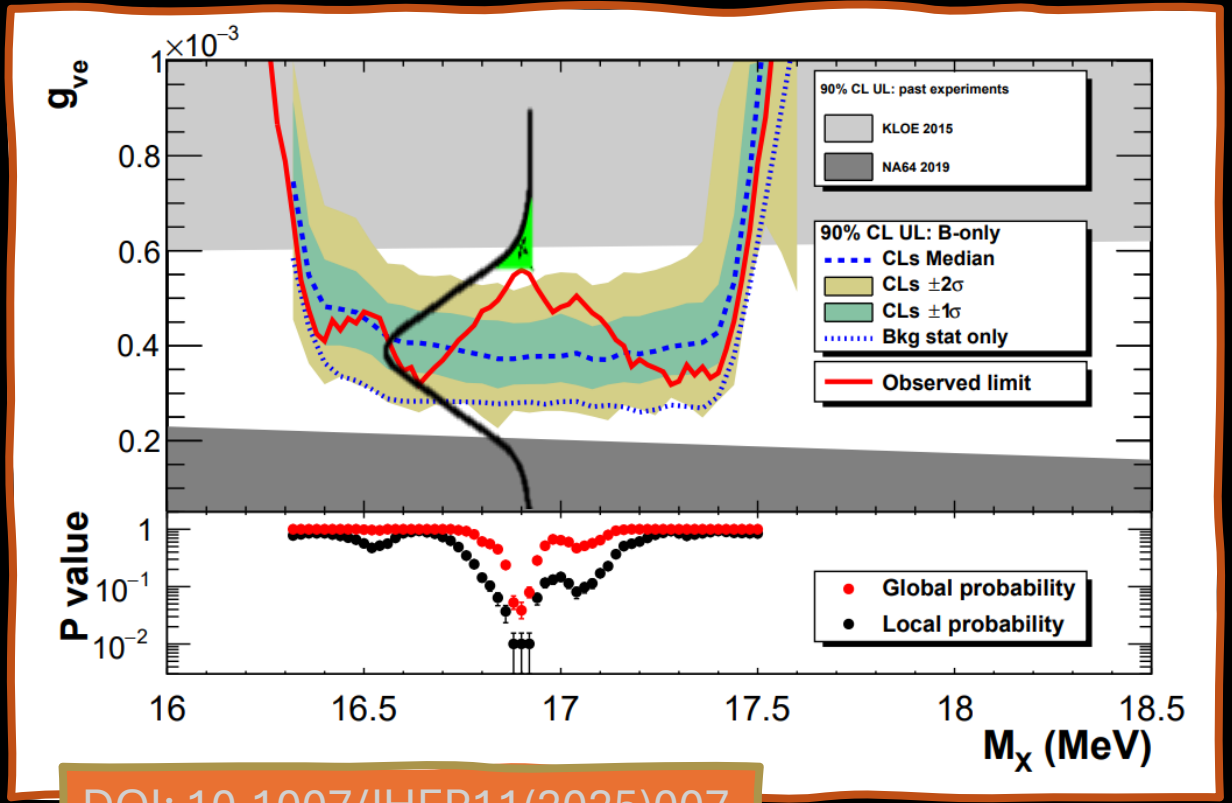

DOI: 10.1007/JHEP11(2025)007

Run III: analysis & uncertainties

Recently PADME collaboration published the results of the Run III analysis.

Evaluating:

$$g_R(s) = \frac{N_2(s)}{N_{bkg}(s)} = \frac{N_2(s)}{N_{POT}(s)B(s)}$$

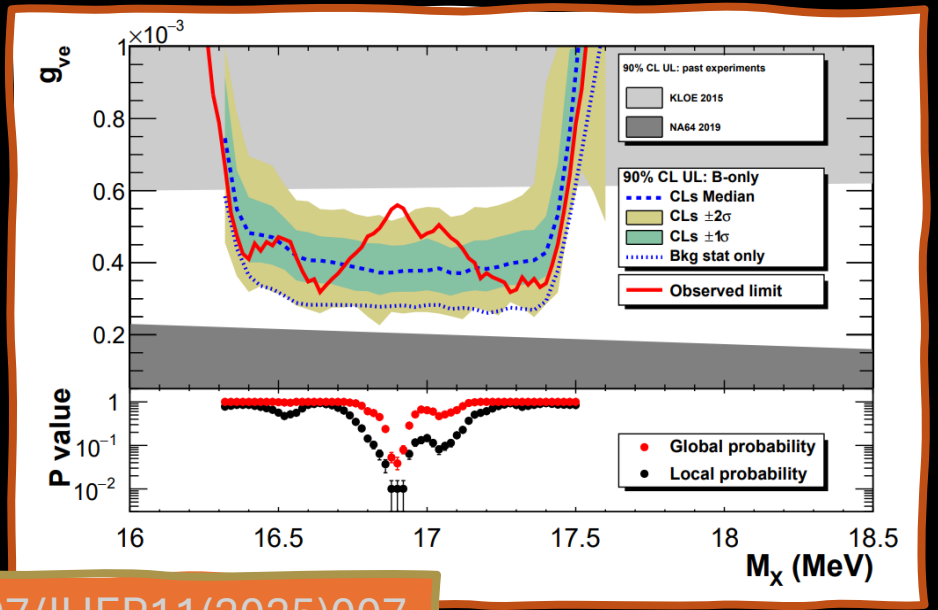

DOI: 10.1007/JHEP11(2025)007

Number of e^+e^- candidates

Number of Positrons On Target

Number of Background

Source	*Error [%]*
N_2	0.6
N_{POT}	0.35
B	0.55
Total on g_R	**0.89**

Background subtraction (bremsstrahlung) + statistics

Beam spread + radiation induced loss

MC statistics + cluster reconstruction efficiency

Upgrade with MICROMEGAS detectors

Run III:

- $N_{PoT} \sim 7 \times 10^{11}$
- Acceptance (~10%)
- Flux measurement & Beam related uncertainties
- Insufficient discrimination between charged/neutral particles from ETag
- Passive material of TimePix

Run IV upgrades:

- Increase the statistics (goal: ~2x N_{PoT})
- New target position (closer to ECAL) → 2x acceptance
- **Gaseous tracking detectors (padMMe and TMM)**
  - → **Discrimination of photons/charged particles**
  - → **Beam monitor capabilities**
- **Improved spatial and angular resolution**
- N_{ee} normalization to **another physical process**, like $N_{\gamma\gamma}$
- Reduced passive material along the beamline

Run IV started in June and ended in November

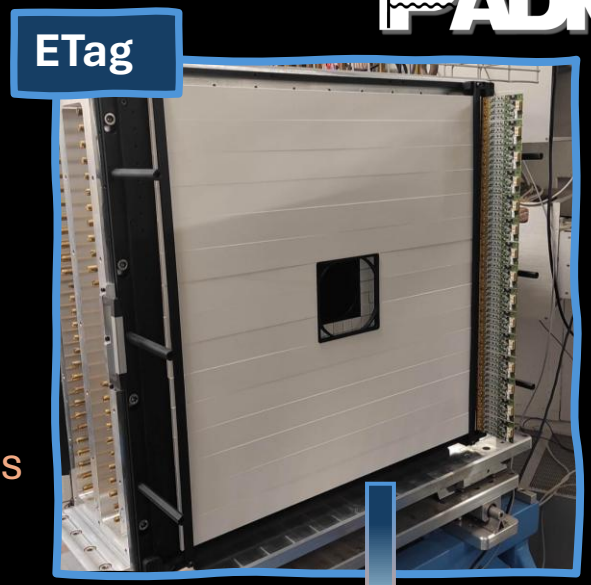

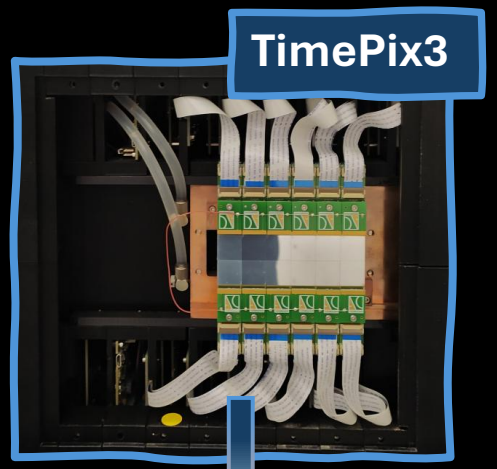

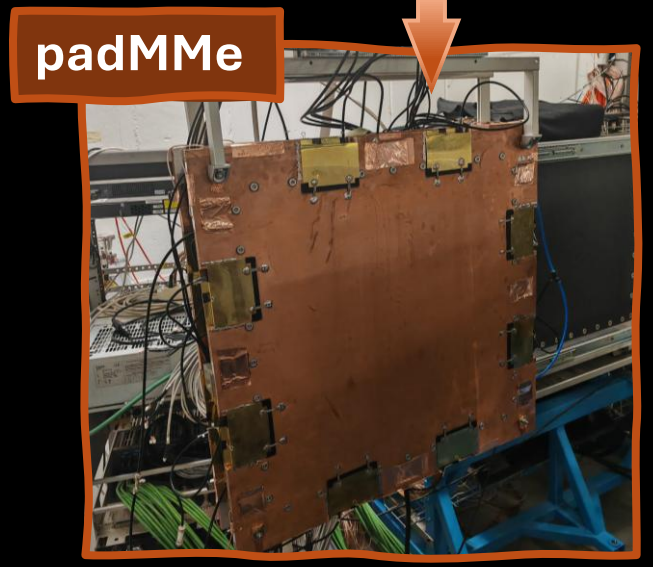

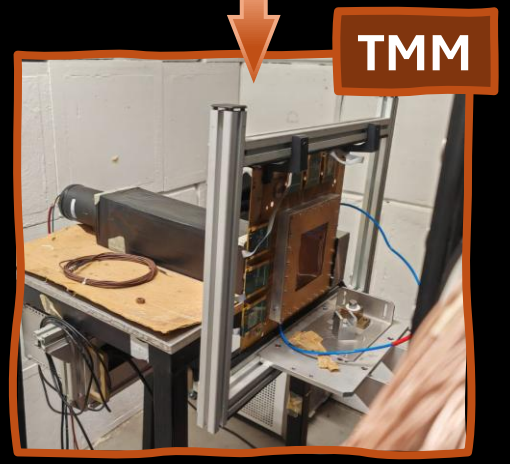

Run IV: prospects

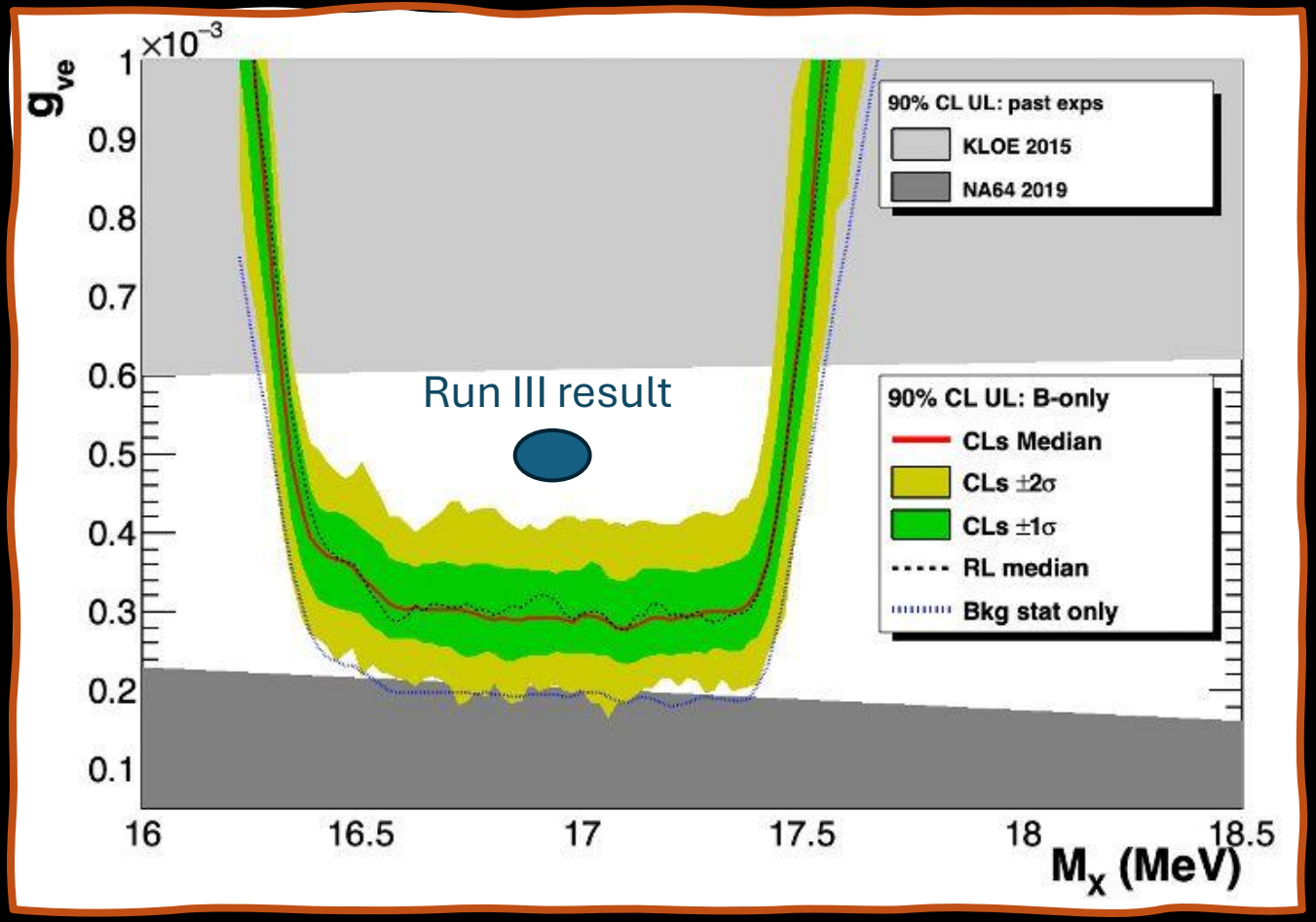

this plot is obtained considering the run3 dataset but with systematic decreased. Namely the full systematic uncertainty is lowered to 0.5%

Gas detectors

All gaseous detector are based on one principle: **when a charged particle passes through a gas it produce couples of ions and electrons.**

The charge is collected using an electric field on electrodes.

→ **Anode for electrons**

→ **Cathode for ions**

Ionization of the medium

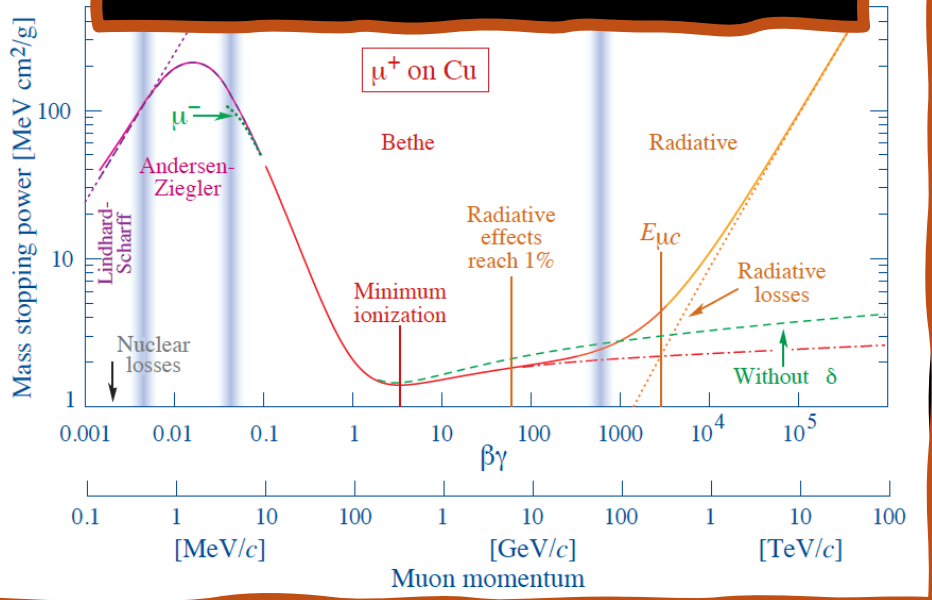

$$\left\langle -\frac{dE}{dx} \right\rangle = K z^2 \frac{Z}{A} \frac{1}{\beta^2} \left[\frac{1}{2} \ln \frac{2 m_e c^2 \beta^2 \gamma^2 W_{\max}}{I^2} - \beta^2 - \frac{\delta(\beta\gamma)}{2} \right]$$

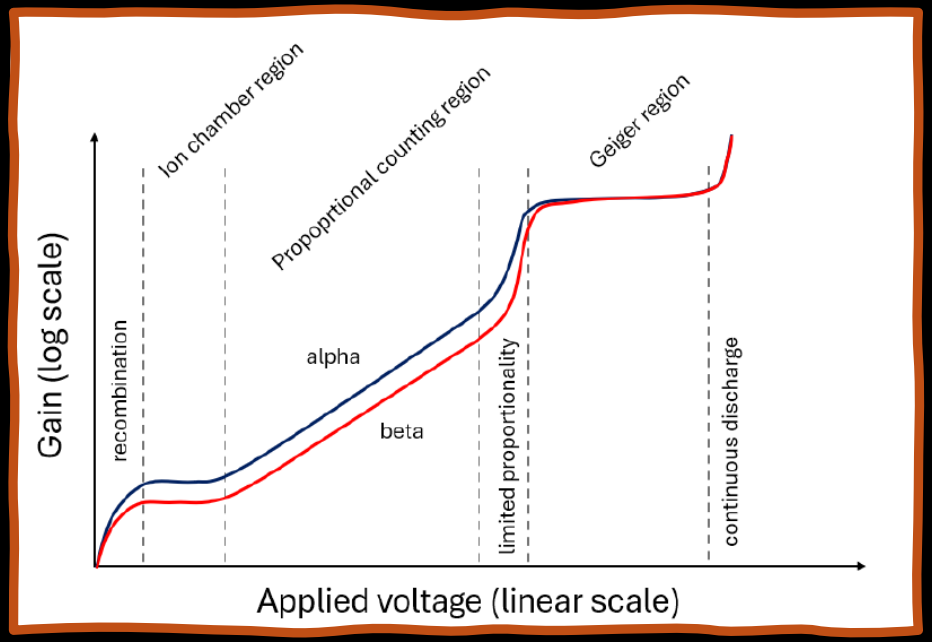

The charge is too small in gas (not in liquid) to be measured

→ Need built in amplification process

Higher is the electric field higher is the energy gained by electrons in the subsequent multiplication process but too high field would make you loose the proportionality regime.

Gas detectors

With respect to the applied voltage on the cathode, one can have different regimes for a gaseous detector:

- **Recombination**:
  the ionized electrons recombines with atoms
  can't see any tracks

- **Ionization chamber region**:
  the charge is not multiplied ,the signal is the ionized charge

- **Proportional counting region**:
  the charge is multiplied linearly through secondary ionizations

- **Geiger region**:
  the high voltage makes the amplification very high, cannot track but can be used to count

- **Continuous discharge**:
  the electric field is too high that creates continuous discharges

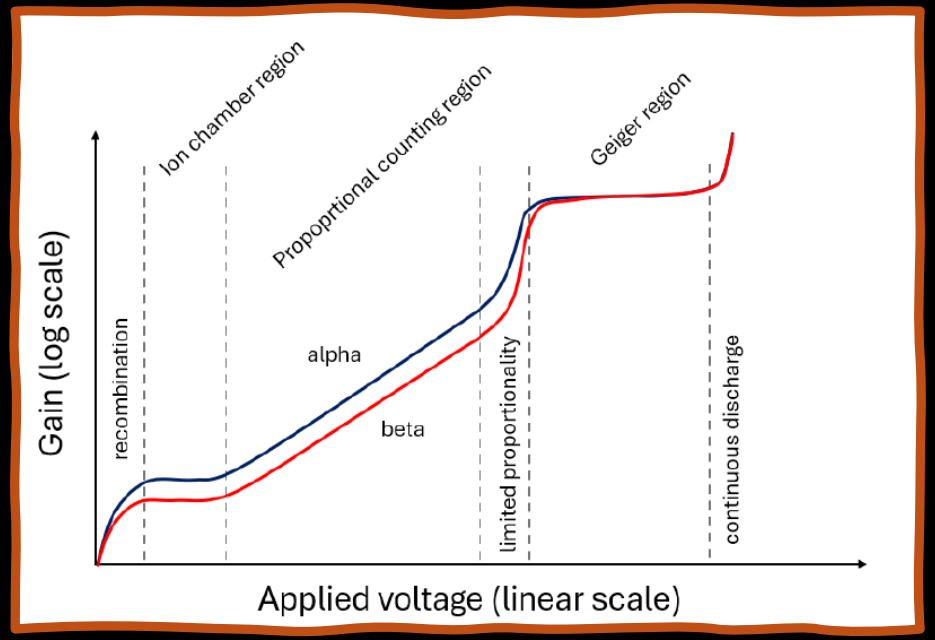

MICROMEGAS: bulk or floating mesh?

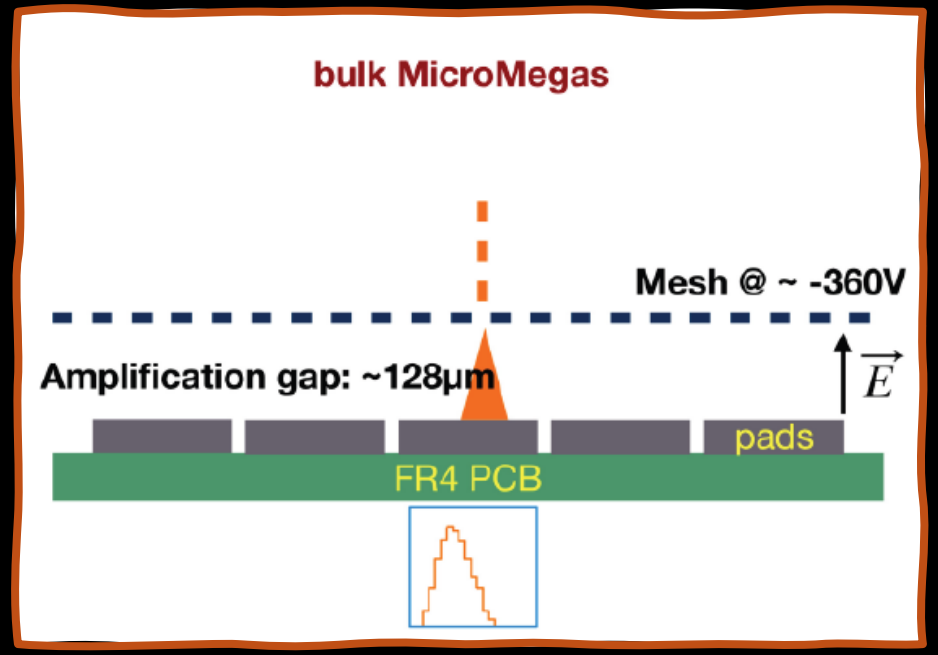

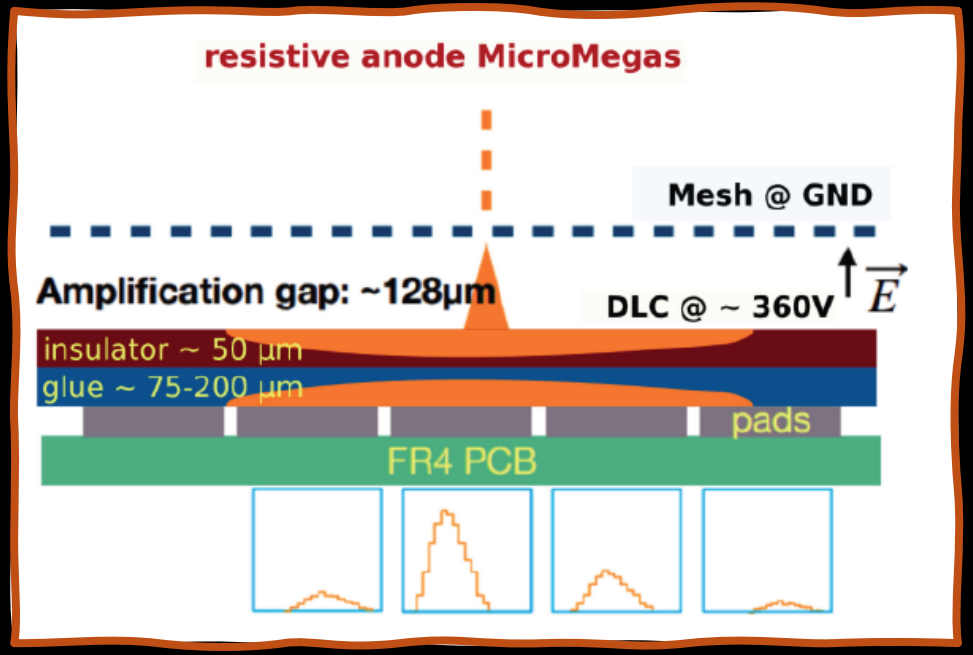

padMMe: gas mixture

Gas	Z	A	ρ (g/cm^3)	E_{ex} (eV)	E_{ion} (eV)	I (eV)	w_i (eV)	$\frac{dE}{dx}$ (MeV cm^2/g)	$\rho\frac{dE}{dx}$ (keV/cm)	n_p (cm^{-1})	n_{tot} (cm^{-1})	X_0 (m)
H_2	2	2	$8.38 \cdot 10^{-5}$	10.8	15.4	19.2	37	4.03	0.34	5.2	9.2	7522
He	2	4	$1.66 \cdot 10^{-4}$	19.8	24.5	41.8	41	1.94	0.32	5.9	7.8	5682
N_2	7	28	$1.17 \cdot 10^{-3}$	8.1	15.6	82	35	1.68	1.96	(10)	56	325
O_2	8	32	$1.33 \cdot 10^{-3}$	7.9	12.1	95	31	1.69	2.26	22	73	257
Ne	10	20.2	$8.38 \cdot 10^{-4}$	16.6	21.6	137	36	1.68	1.40	12	39	345
Ar	18	39.9	$1.66 \cdot 10^{-3}$	11.5	15.8	188	26	1.47	2.44	29.4	94	118
Kr	36	83.8	$3.49 \cdot 10^{-3}$	10.0	14.0	352	22	1.33	4.64	31.6	192	33
Xe	54	131.3	$5.49 \cdot 10^{-3}$	8.4	12.1	482	22	1.23	6.76	44	335	15
CO_2	6,8	44	$1.86 \cdot 10^{-3}$	5.2	13.8	85	35	1.62	3.01	35.5	91	183
CH_4	6,1	16	$7.1 \cdot 10^{-4}$	9.8	15.2	41.7	28	2.21	1.48	25	53	640
C_2H_6	6,1	30	$1.34 \cdot 10^{-3}$	8.7	11.7	45.4	27	2.30	3.08	41	111	340
i-C_4H_{10}	6,1	58	$2.59 \cdot 10^{-3}$	6.5	10.8	48.3	34	2.86	7.39	84	195	169
CF_4	6,9	88	$3.78 \cdot 10^{-3}$	12.5	15.9	115	34.3	1.69	6.37	51	108	92
C_2H_6O (DME)	6,1,8	46	$2.2 \cdot 10^{-3}$	6.4	10.0	60	23.9	1.77	3.9	55	160	222

88%

2%

10%

padMMe: segmentation designs

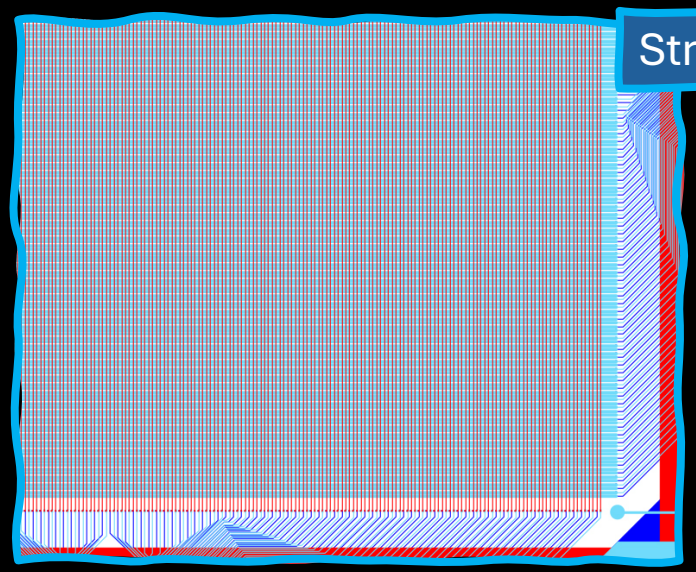

Straight strips

The x and y coordinates each are read by parallel Copper strips, separated by 1.2 mm pitch, which guarantee a spatial resolution of ~ 300μm on the layer facing the amplification gap. On the other layer, that gives the second coordinate, the resolution worsen to ~ 1 mm, due to the induced charge from the upper layer strips (capacitive coupling).

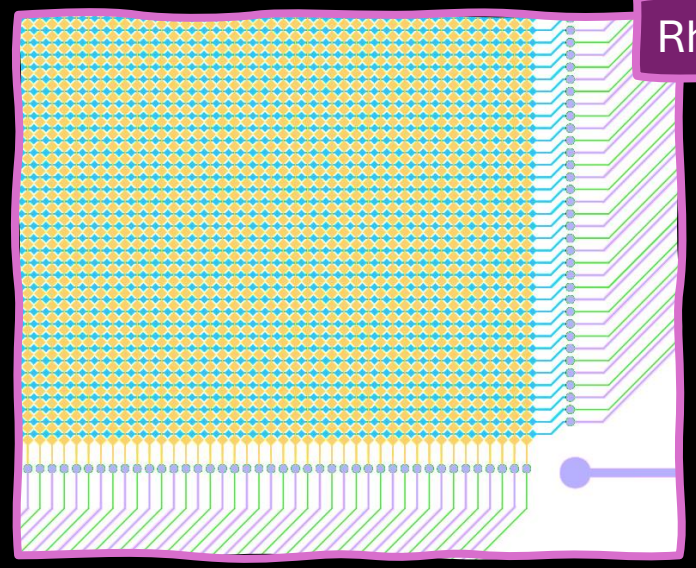

Rhomboidal strips

The reading layers are composed of rhomboidal shaped strips, always with a pitch of 1.2 mm. The two layers are shifted one to the other in such a way as not to overlap the x and y readout pads. This technology minimizes the capacitive coupling between the two layers, keeping the resolution on each coordinate of ~ 300 μm. The pads have different areas, 0.49 mm^2 for the upper layer and 0.25 mm^2 for the down layer, making the capacitive coupling to the resistive layer the same for both the readout layers. Anyway, such difference in surfaces of the pads causes a difference of ~ 20% for the collected charge of the two layers.

padMMe: noise and Faraday cage

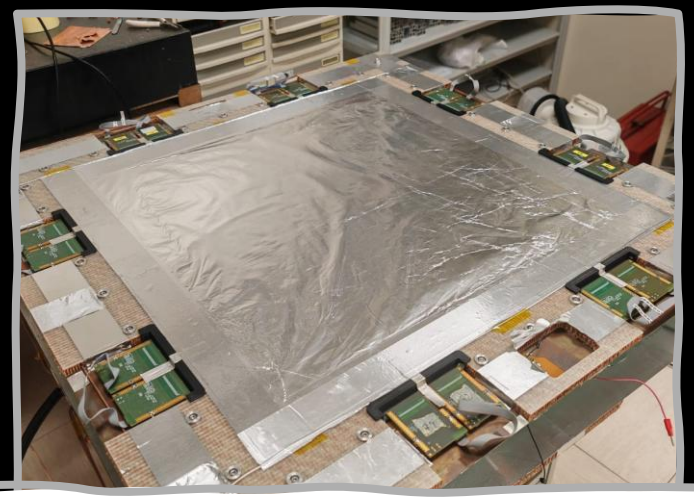

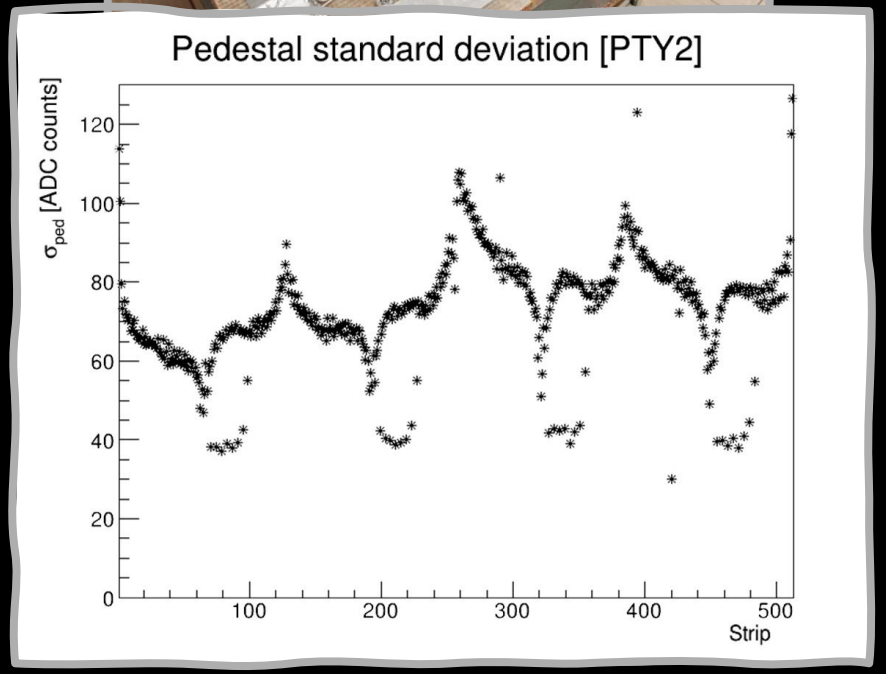

VS

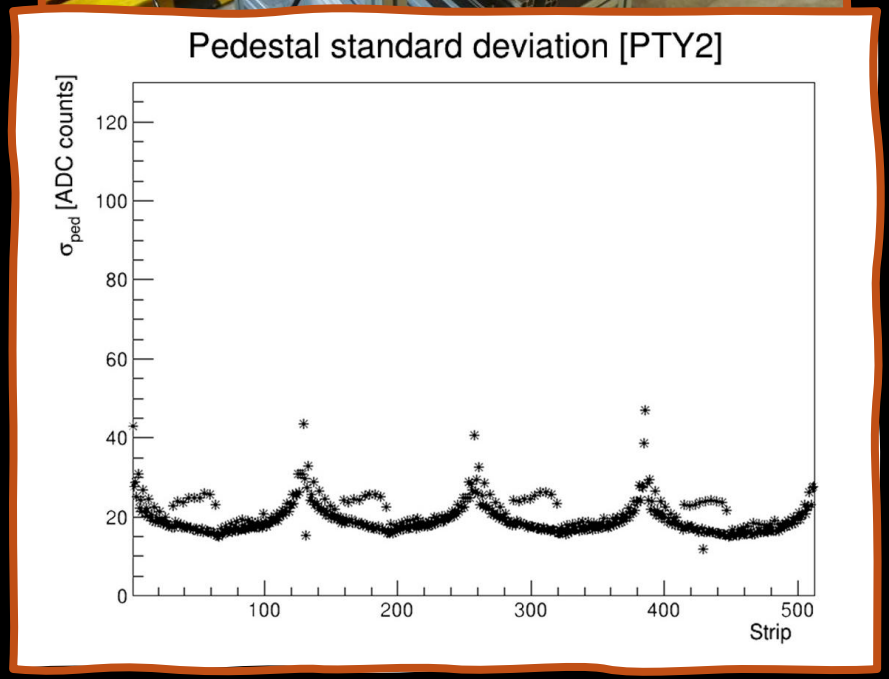

padMMe: dimensional measurements

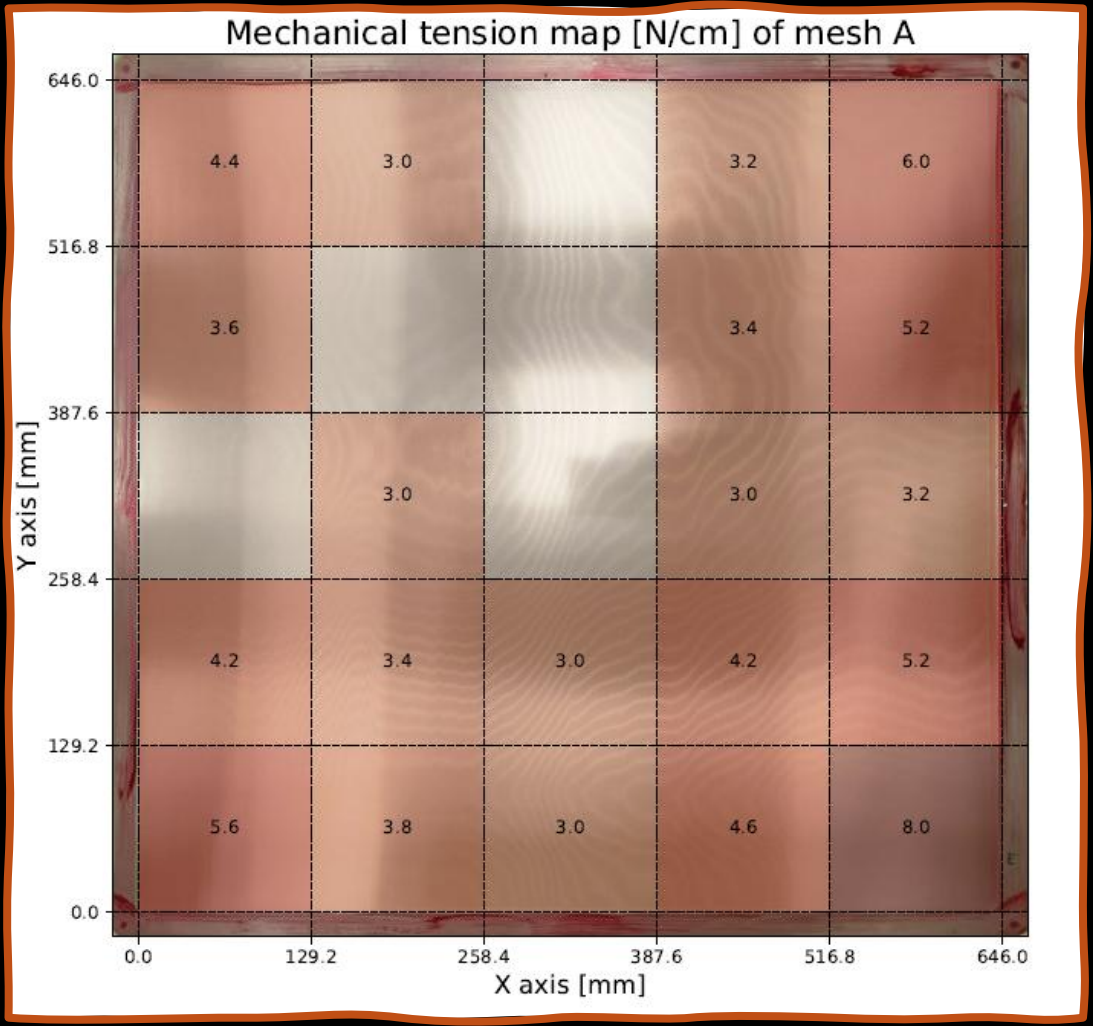

Pillar height

padMMe: deformation of readout panel

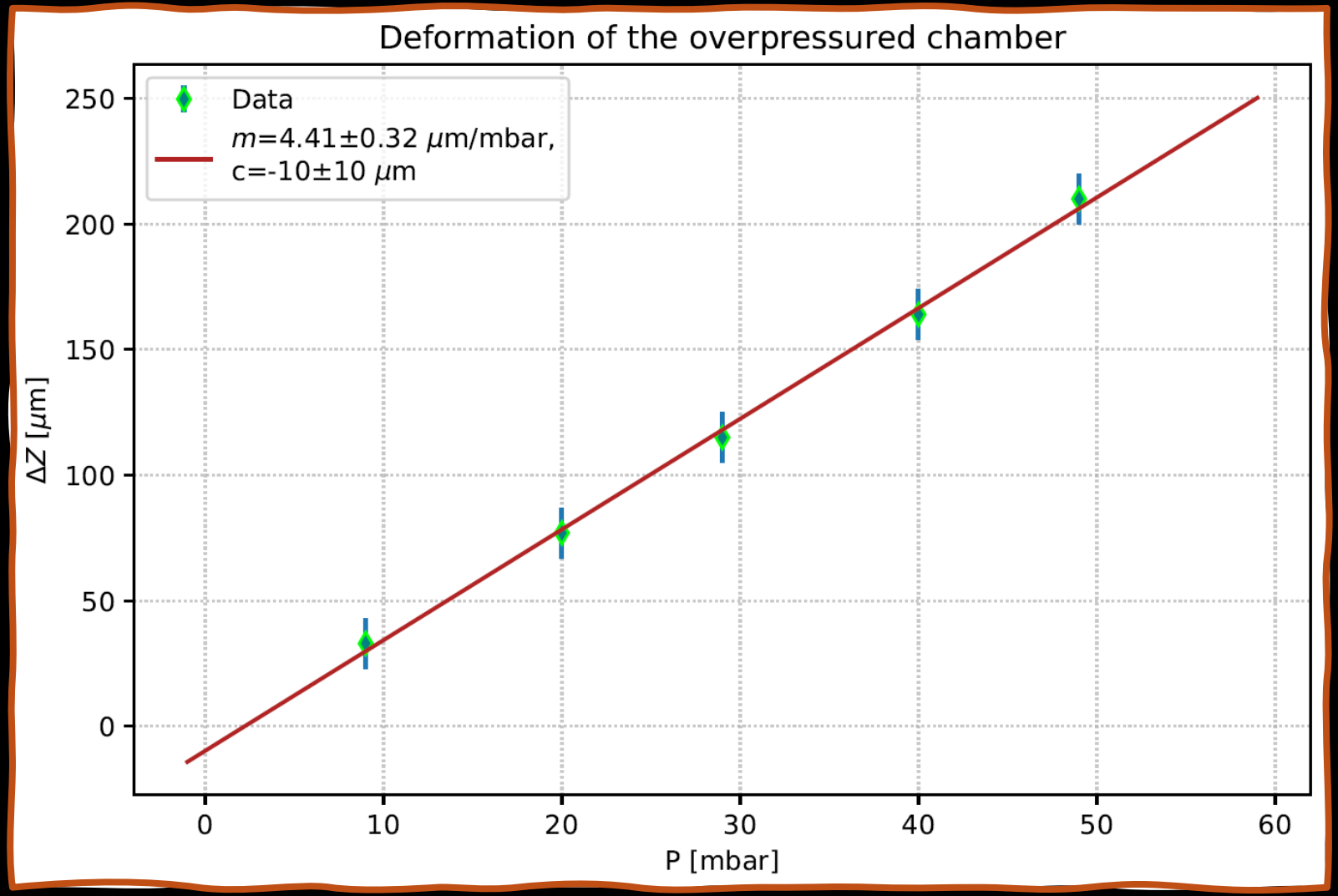

padMMe: gas tightness

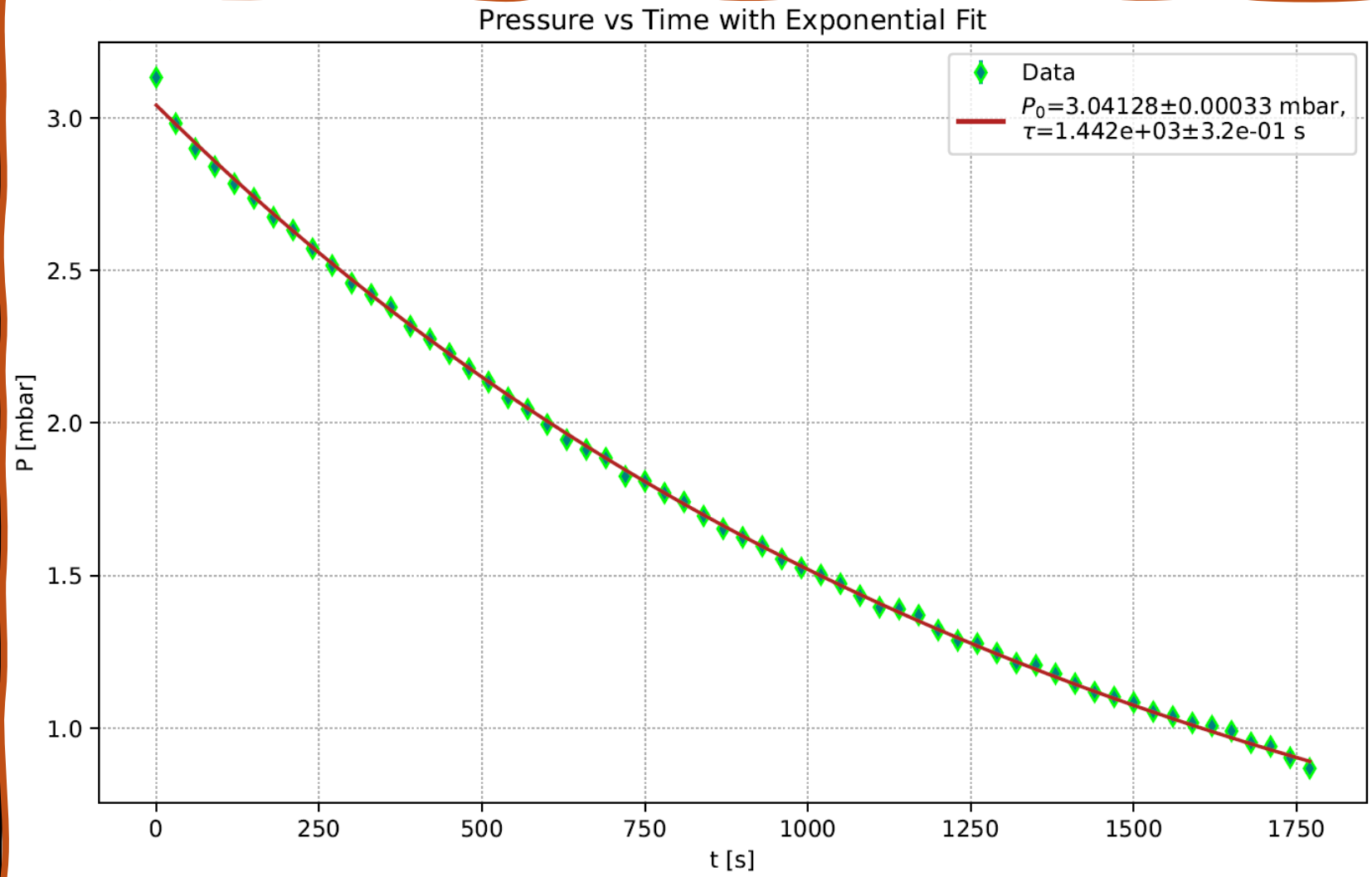

Time of tightness:

$$\tau = (1442.00 \pm 0.32)\ \mathrm{s} \simeq 24\ \mathrm{min.}$$

Volume leakage:

$$\frac{V}{\tau} = (0.8989 \pm 0.0020)\ \mathrm{L/h}$$

padMMe: HV study stability

Operating in PADME @490V

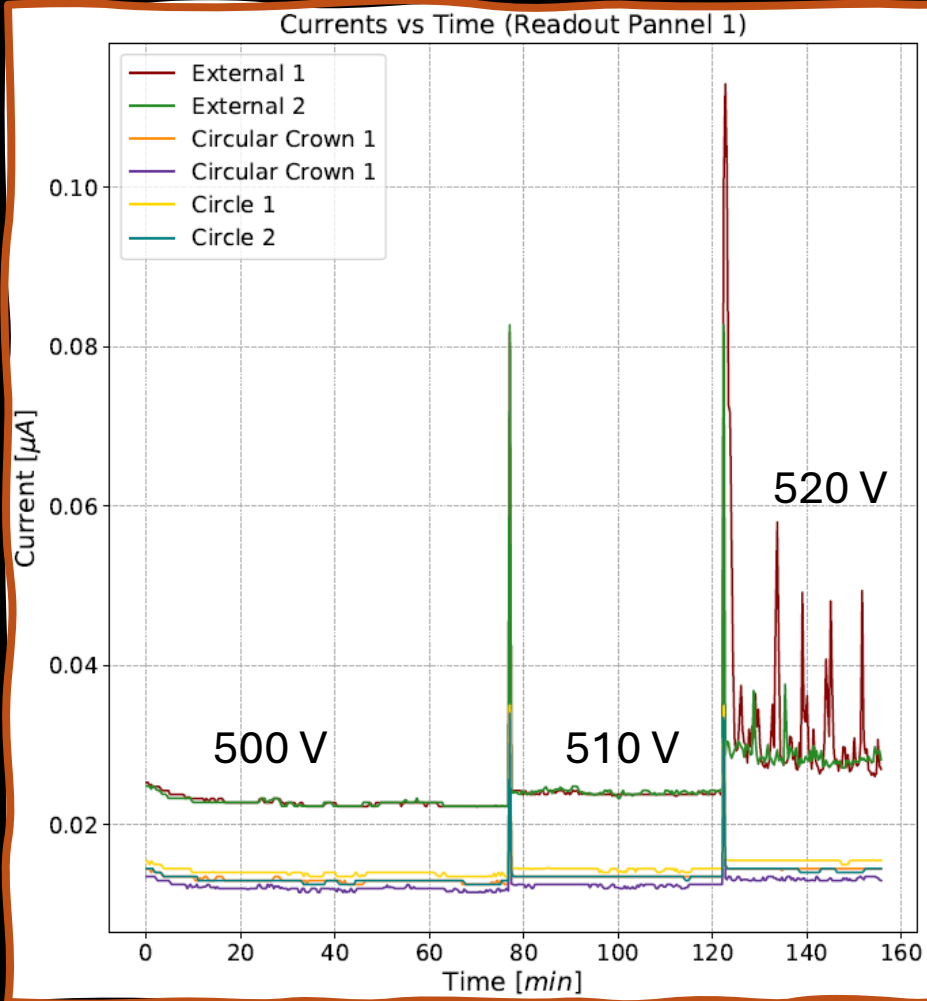

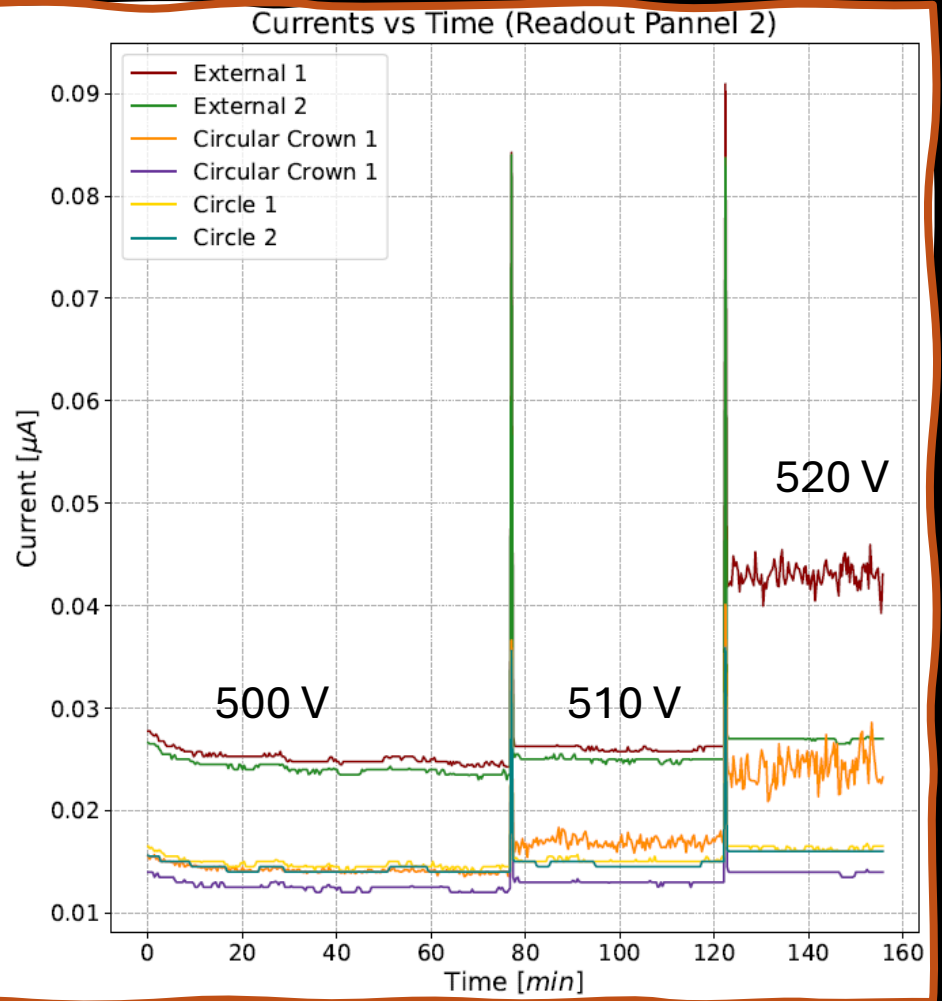

padMMe: collected charge spectrum

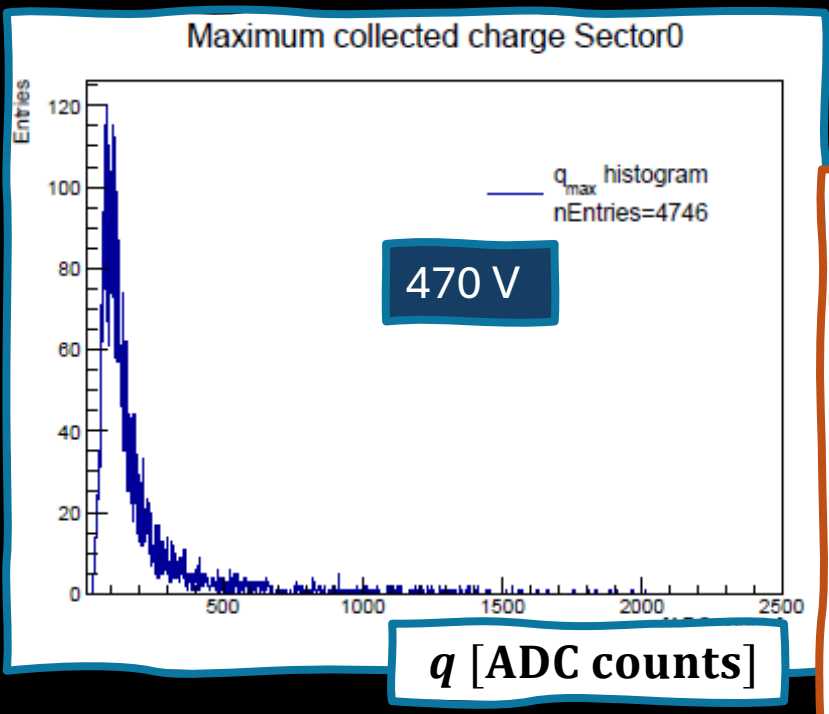

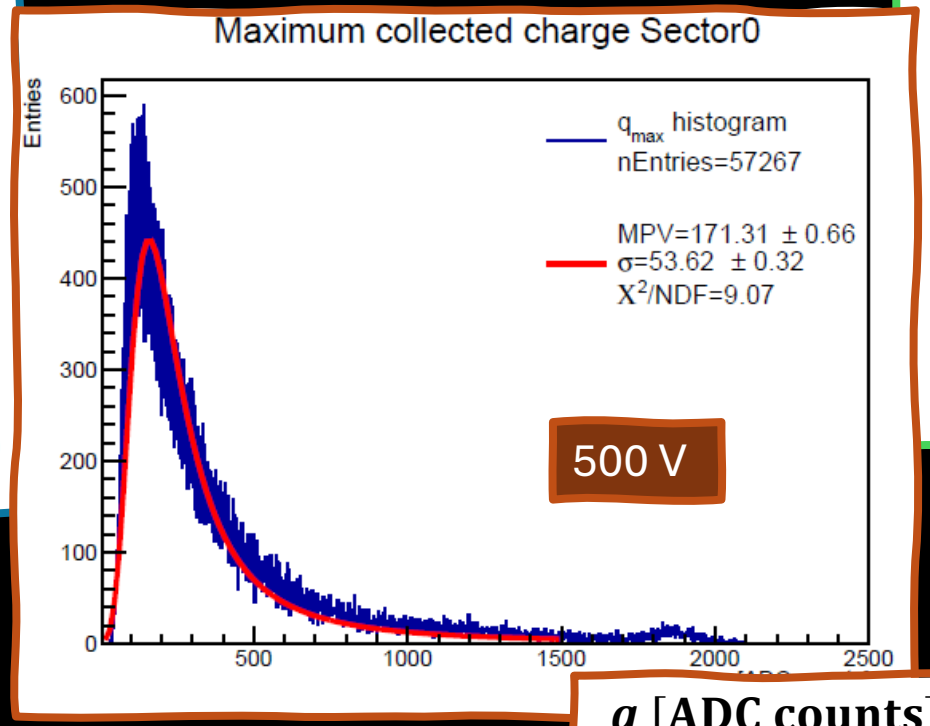

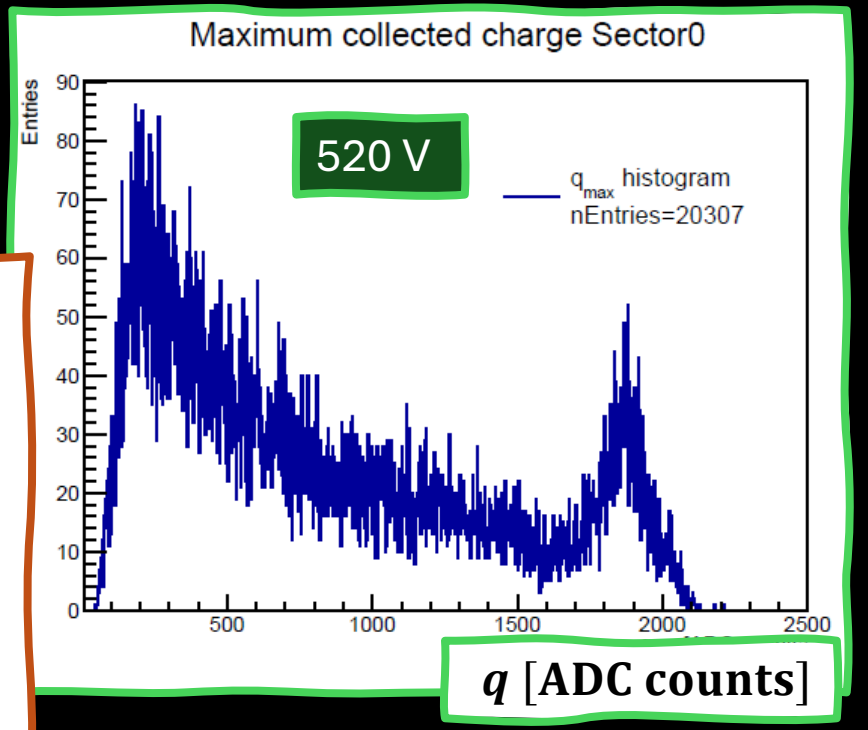

padMMe: gain curve

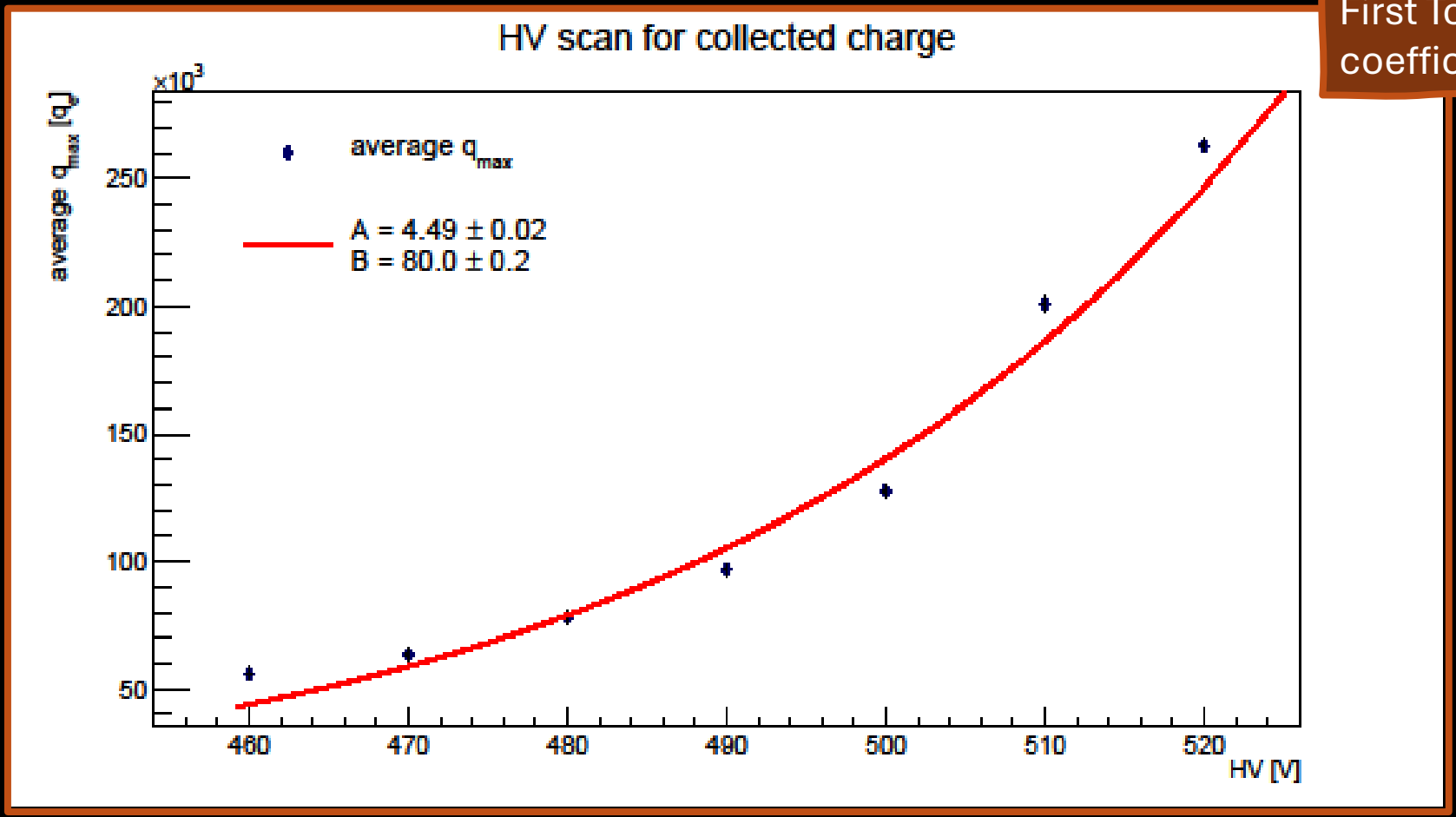

First Townsend coefficient

$$\alpha = Ape^{-\frac{Bpd}{V}}$$

Pressure: $p \sim 1\ bar \sim 750\ mmHg$
Amplification gap: $d = 128\ \mu m$
Applied voltage: V

At $V = 500\ V$ we found:

Gain = $e^{\alpha d} \sim 10^4$

padMMe @ CRS: reconstruction

$$X \text{ or } Y = \#ch * p + \Delta_{sectors}$$

$$t_{drift} = t_{mean} - t_0$$

Mean time of the signal (charge-weighted average)

From time calibration

$$\begin{aligned} \text{TOP panel:} \quad & Z = d - Z_{corr} - t_{drift} \cdot v_{drift} \\ \text{BOTTOM panel:} \quad & Z = -d + t_{drift} \cdot v_{drift} + Z_{corr} \end{aligned}$$

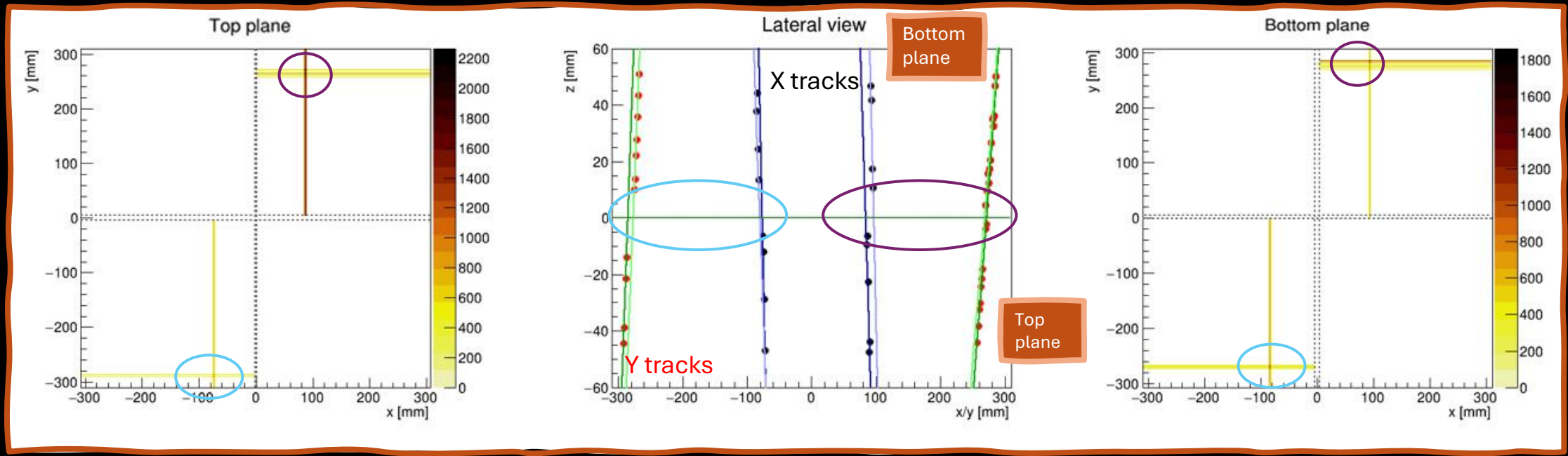

padMMe @ CRS: reconstruction

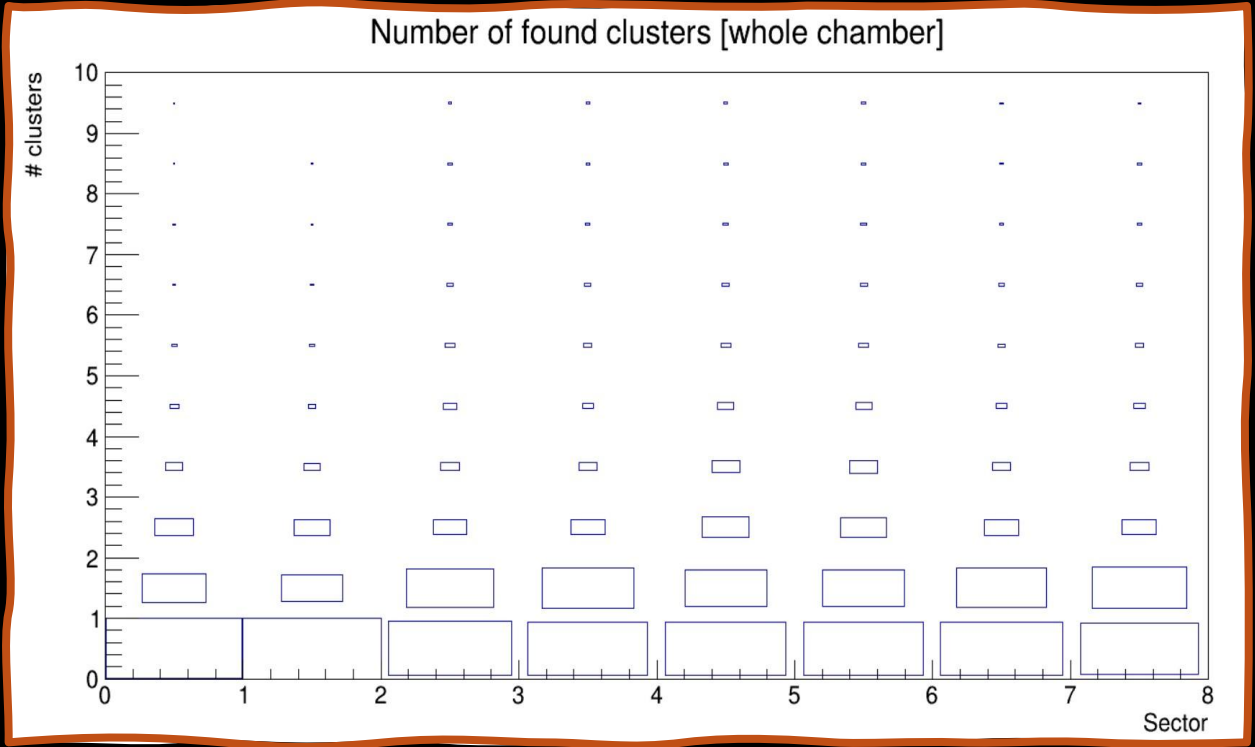

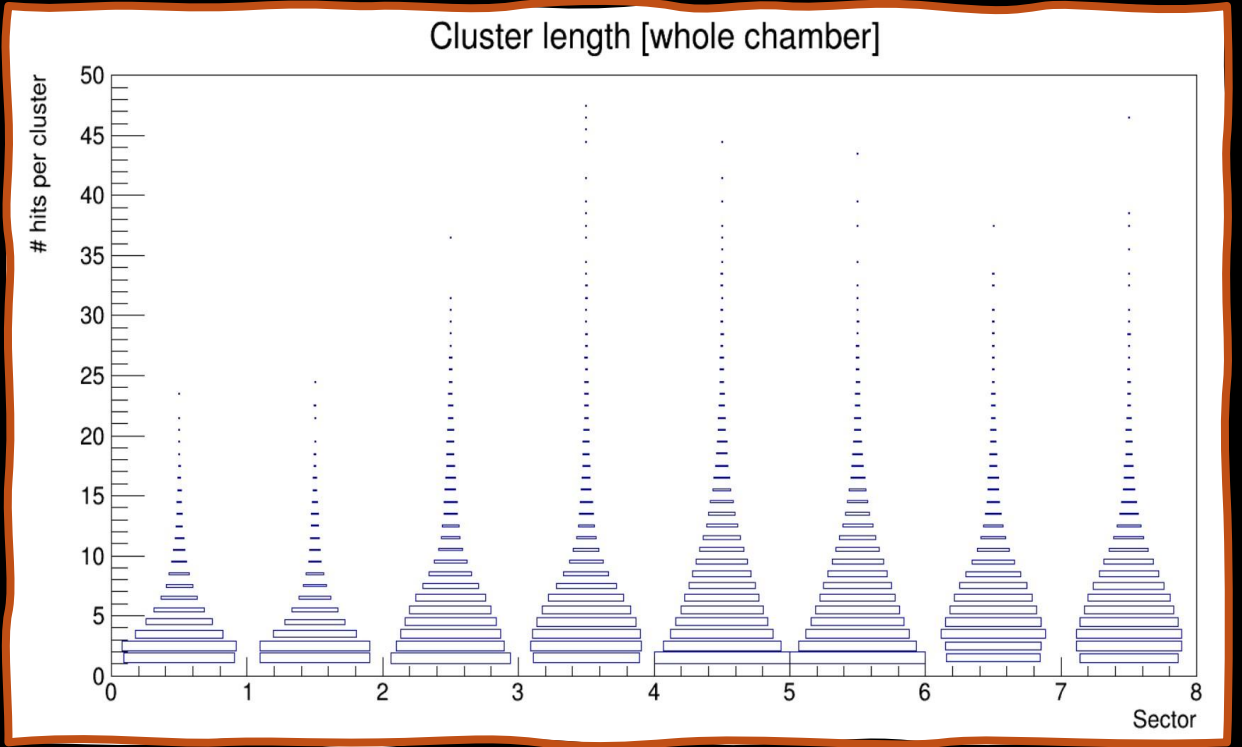

padMMe @ CRS: reconstruction

For angled tracks: $x = m \cdot z + c,$

For vertical tracks: (centroid) $m = 0$ $c = \sum_i \frac{x_i \cdot q_i}{q_{tot}}$

Plane matching condition:

$$|m_1 - m_2| < 0.5 \text{ rad},$$
$$|c_1 - c_2| < 2 \text{ mm}.$$

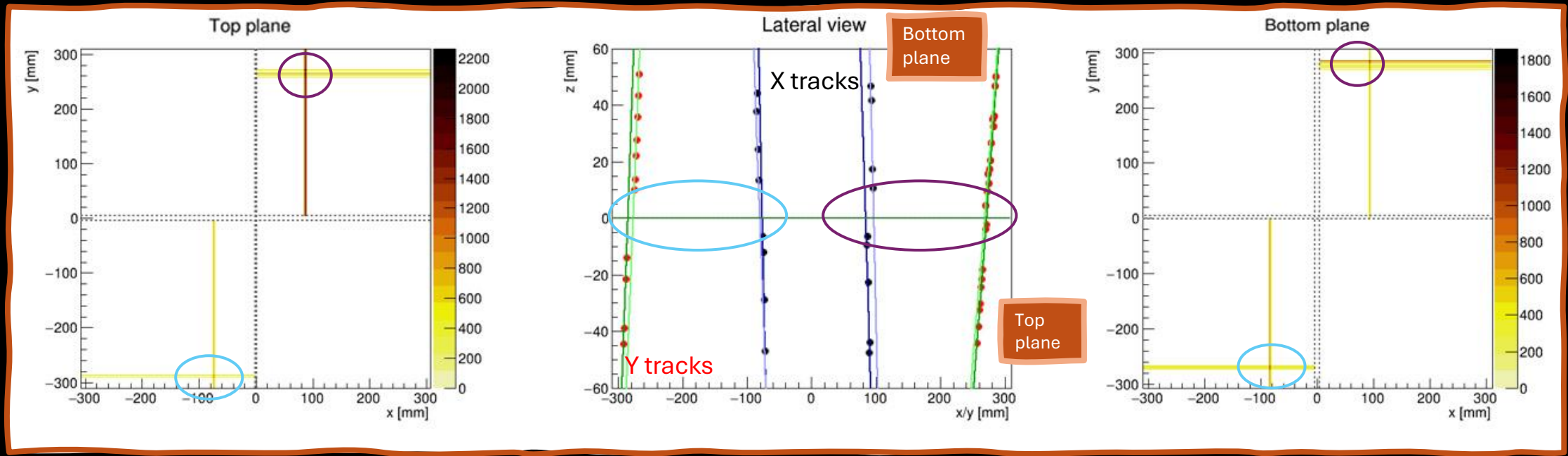

padMMe @ CRS: reconstruction

We calibrate the time, finding the t_0 for each APV chip.

We checked that the readout strips were aligned (no offset between them)

We observed a slewing (time walk) effect.

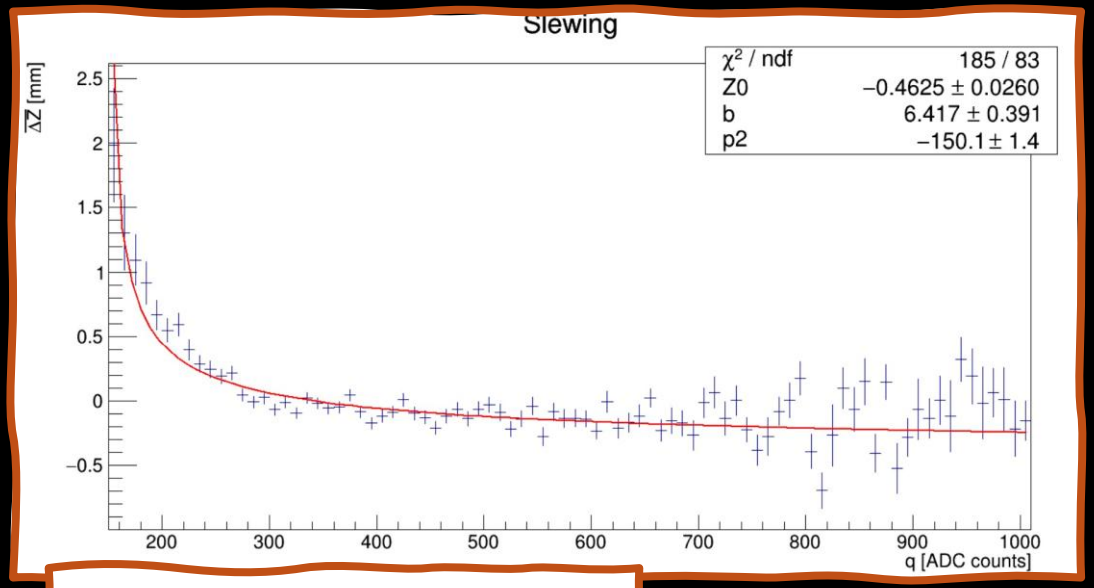

$$\overline{\Delta Z}(q) = Z_0 + \frac{a}{\sqrt{q+b}}$$

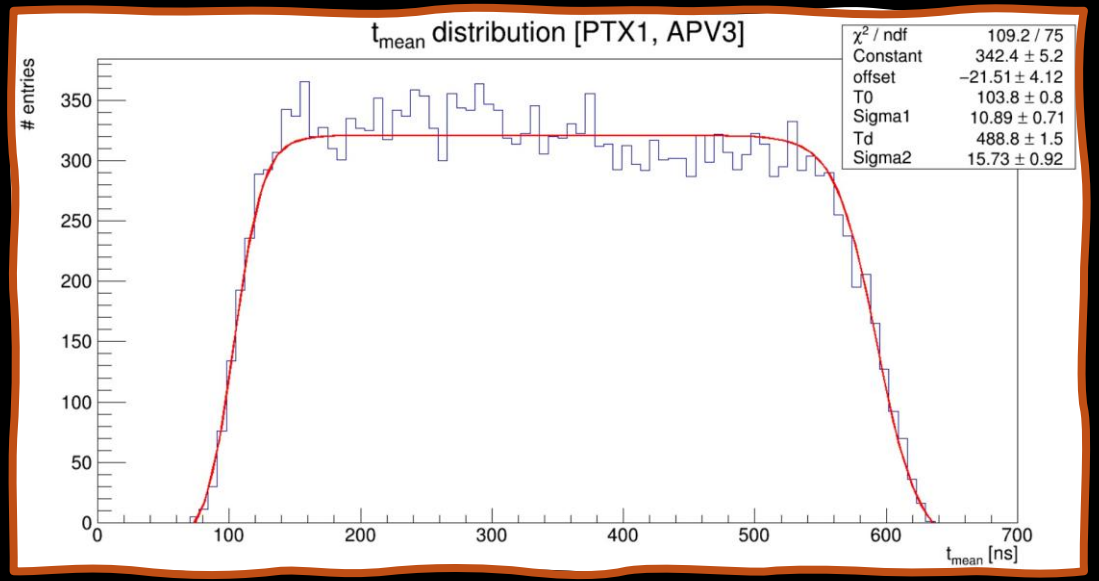

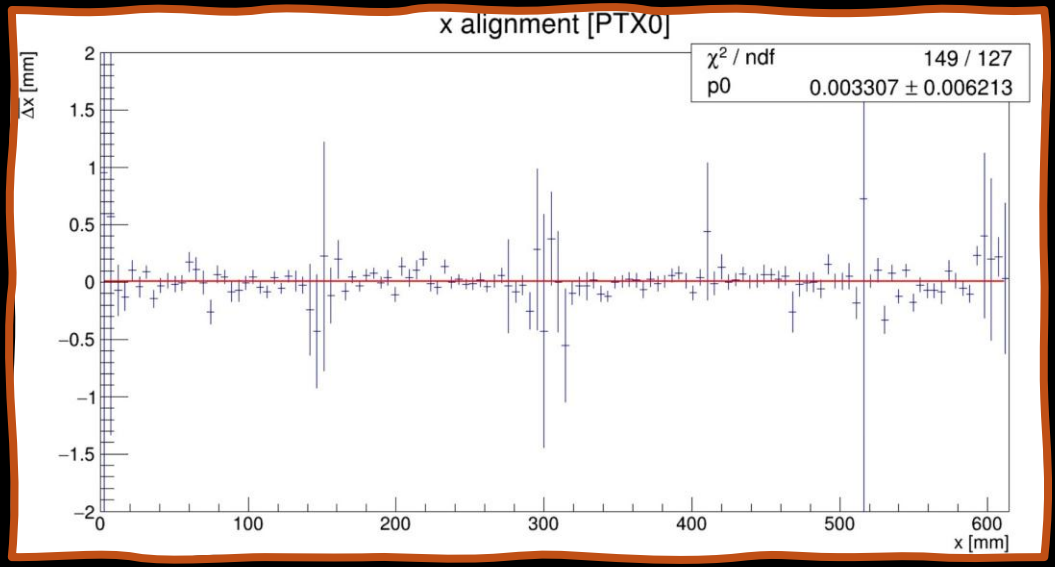

padMMe @ CRS: resolutions

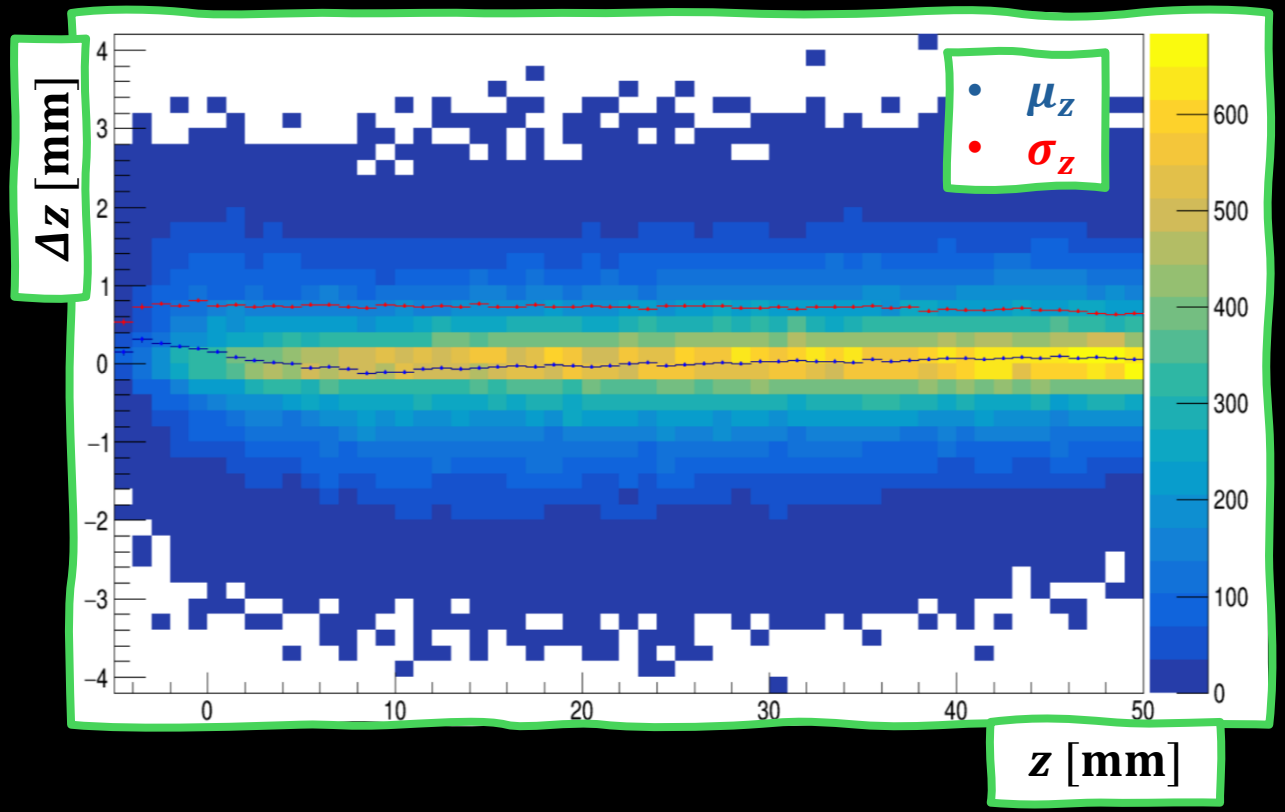

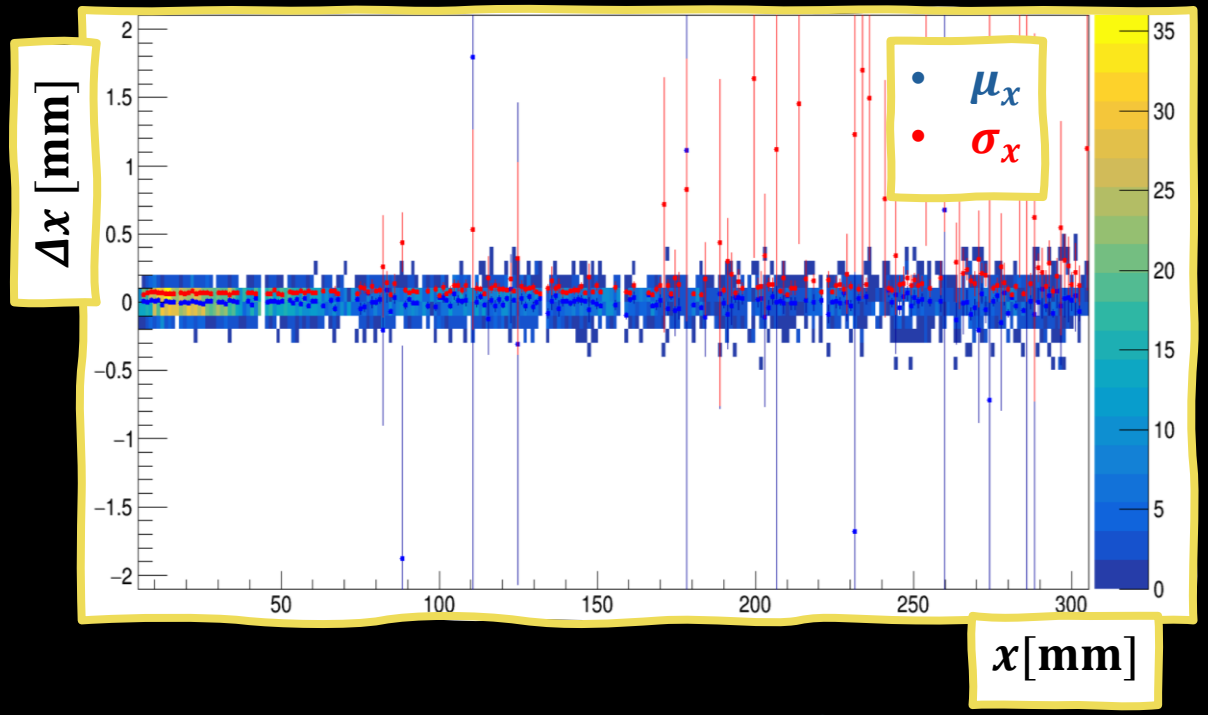

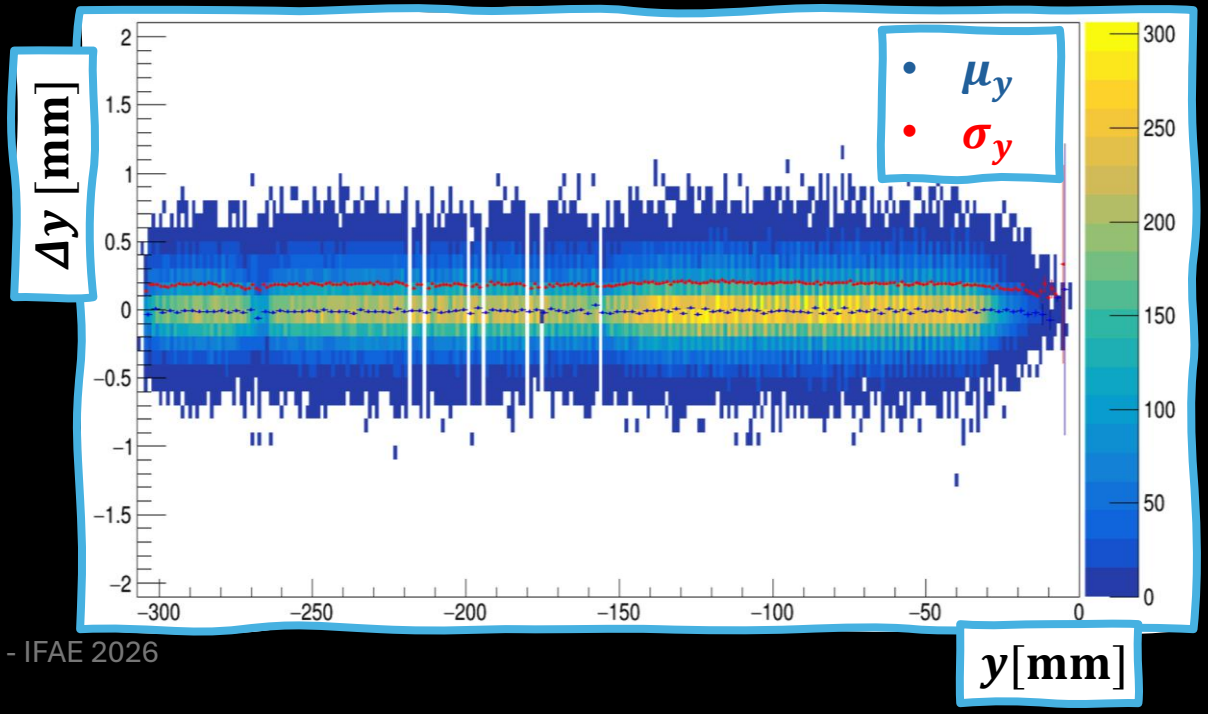

padMMe @ BTF: installation

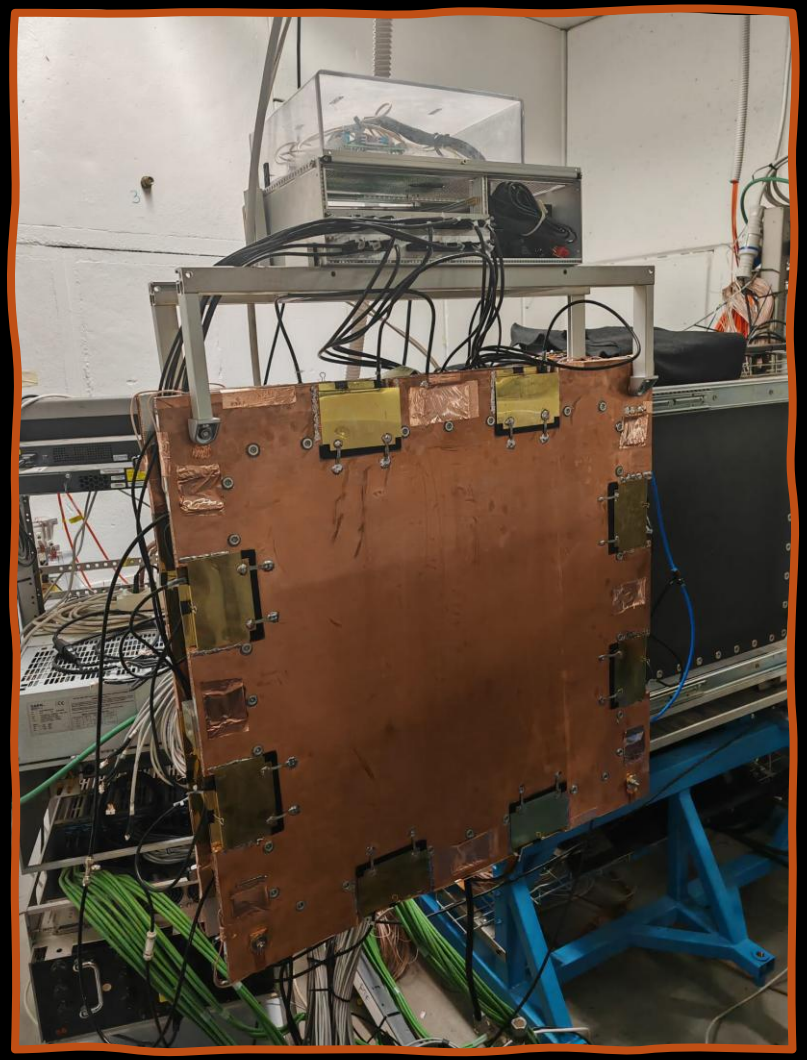

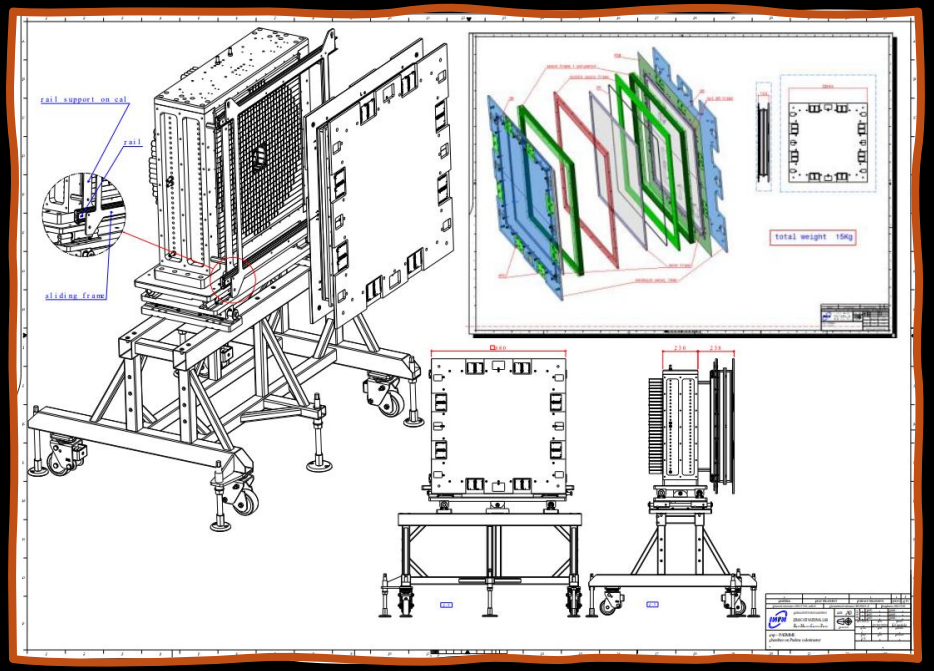

PADME Run IV layout

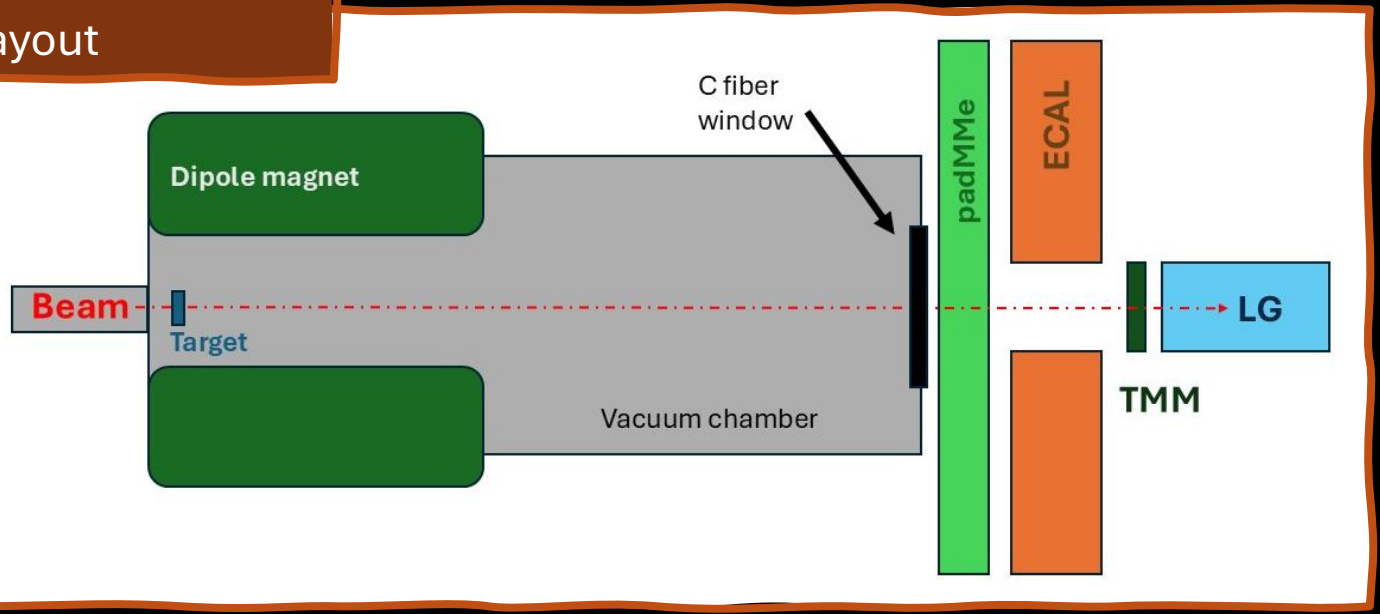

padMMe @ BTF: alignment with Strumento

Made by LNF metrology team

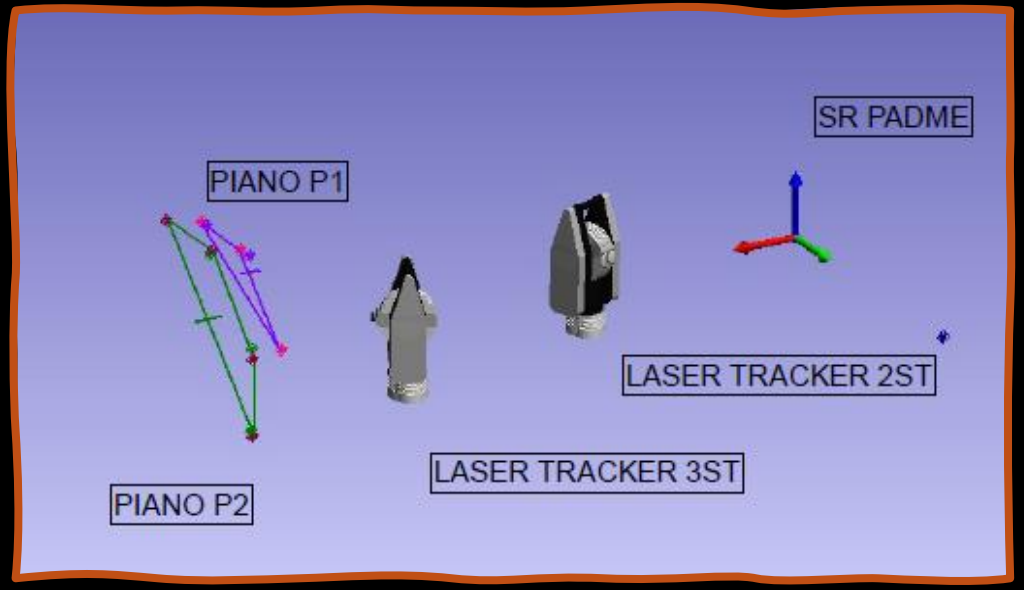

Mire P1

Point Group C::P1							
Point Name	X (mm)	Y (mm)	Z (mm)	Ux (mm)	Uy (mm)	Uz (mm)	Mag (mm)
P1XT0	2348.17	-102.12	450.33	0.01	0.01	0.01	0.02
P1XT1	2350.70	210.35	445.23	0.01	0.01	0.01	0.02

Plane Relationship C::Piano P1	
Criteria	Measured
Flatness	0.00
Centroid X	2357.32
Centroid Y	151.74
Centroid Z	355.83
RMS	0.00
Measurements	3

Piano P1

Point Group C::Piano P1							
Point Name	X (mm)	Y (mm)	Z (mm)	Ux (mm)	Uy (mm)	Uz (mm)	Mag (mm)
1	2348.23	-138.25	453.27	0.01	0.01	0.01	0.02
2	2350.76	145.65	443.27	0.01	0.01	0.01	0.02
3	2353.94	447.97	170.91	0.01	0.01	0.01	0.02

Mire P2

Point Group B::P2							
Point Name	X (mm)	Y (mm)	Z (mm)	Ux (mm)	Uy (mm)	Uz (mm)	Mag (mm)
P2S0	2467.89	434.66	-115.94	0.01	0.01	0.01	0.02
P2S1	2467.21	436.00	191.56	0.01	0.01	0.01	0.02
P2XT1	2463.81	127.42	441.83	0.01	0.01	0.01	0.02

Plane Relationship C::Piano P2	
Criteria	Measured
Flatness	0.39
Centroid X	2458.22
Centroid Y	204.15
Centroid Z	233.21
RMS	0.16
Measurements	4

Piano P2

Point Group B::Piano P2							
Point Name	X (mm)	Y (mm)	Z (mm)	Ux (mm)	Uy (mm)	Uz (mm)	Mag (mm)
1	2460.91	-196.56	457.79	0.01	0.01	0.01	0.02
2	2463.36	132.07	455.15	0.01	0.01	0.01	0.02
3	2466.86	437.55	154.66	0.01	0.01	0.01	0.02
4	2467.15	443.34	-134.70	0.01	0.01	0.01	0.02

TMM @ BTF: beam monitoring

A smaller Micromegas chamber (TMM) replaced the TimePix for beam monitoring before the LeadGlass in Run IV.

The TMM is a bulk Micromegas, with and active area of 10x10 cm^2, with a drift gap of 5 mm and an amplification gap of 128 μm. The strips are orthogonal, for X and Y readout and the pitch is 250 μm.
The TMM is kept in the ionization chamber regime (readout 300V, drift -300V)

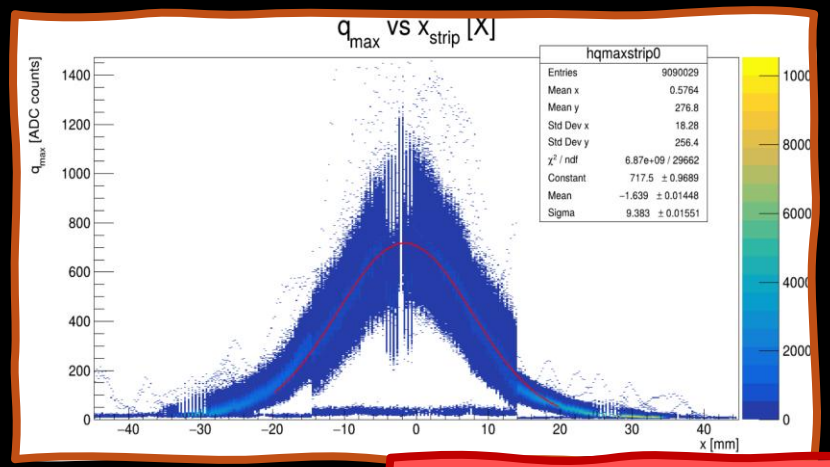

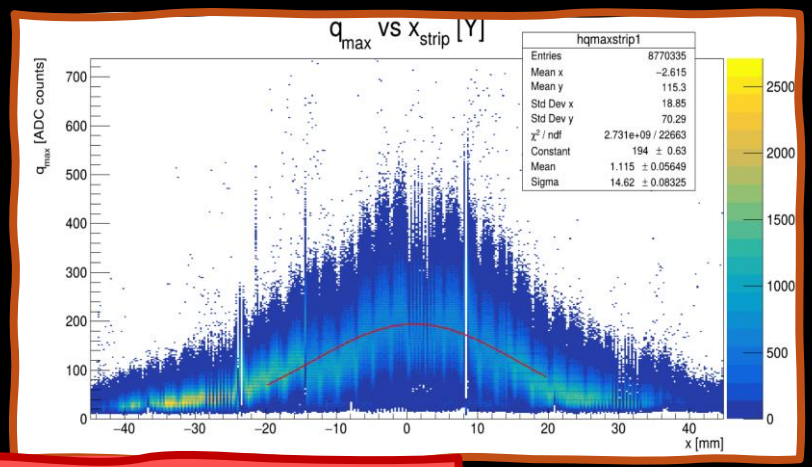

Measured beam spread: $\sim 9 \times 14\ mm^2$

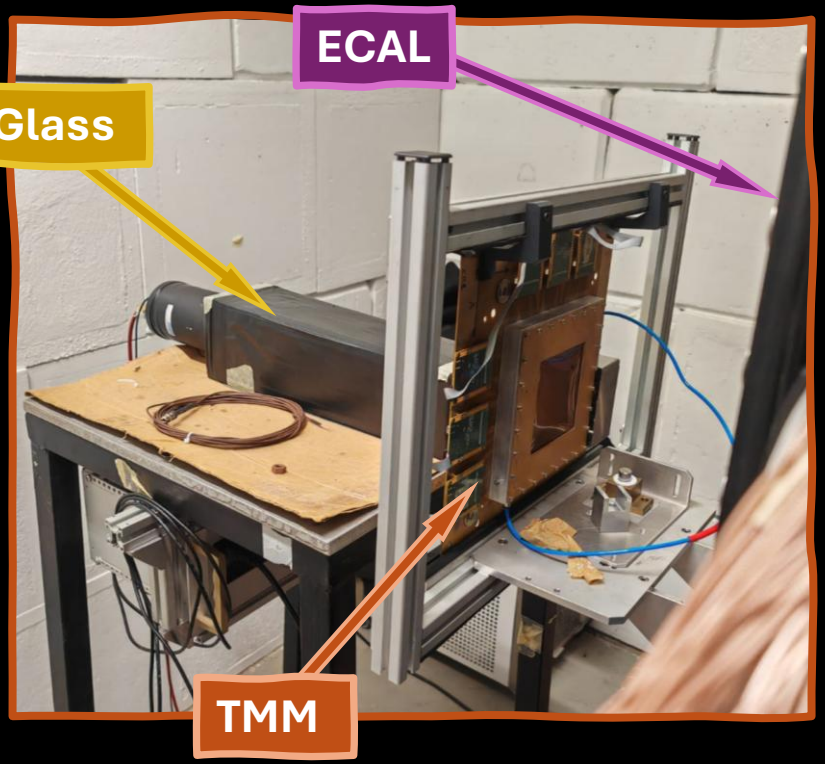

We can measure the beam in three points: target, padMMe and TMM.

We can determine well beam properties, such as direction and spread.

TMM @ BTF: alignment

For the TMM the positioning and alignment is done in the same way of padMMe, using two aims → one for the position, the other for alignment

The real position of the aims was measured using the laser tracker, with respect to the PADME reference system

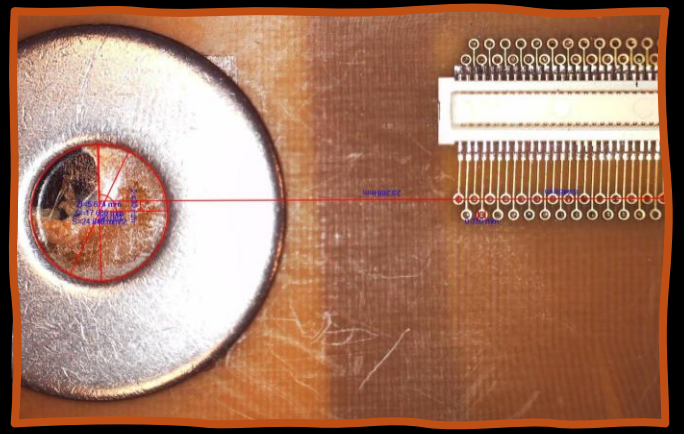

PIANO TMM sfera 1.5

Point Group A::Piano TMM 1.5							
Point Name	X (mm)	Y (mm)	Z (mm)	Ux (mm)	Uy (mm)	Uz (mm)	Mag (mm)
1	3384.59	-129.95	129.45	0.01	0.01	0.01	0.02
2	3384.53	-128.15	84.84	0.01	0.01	0.01	0.02
3	3381.00	123.04	-63.21	0.01	0.01	0.01	0.02

TMM sfera 1.5

Point Group A::TMM 1.5							
Point Name	X (mm)	Y (mm)	Z (mm)	Ux (mm)	Uy (mm)	Uz (mm)	Mag (mm)
1	3380.68	101.69	130.26	0.01	0.01	0.01	0.02
2	3378.80	131.48	-97.78	0.01	0.01	0.01	0.02

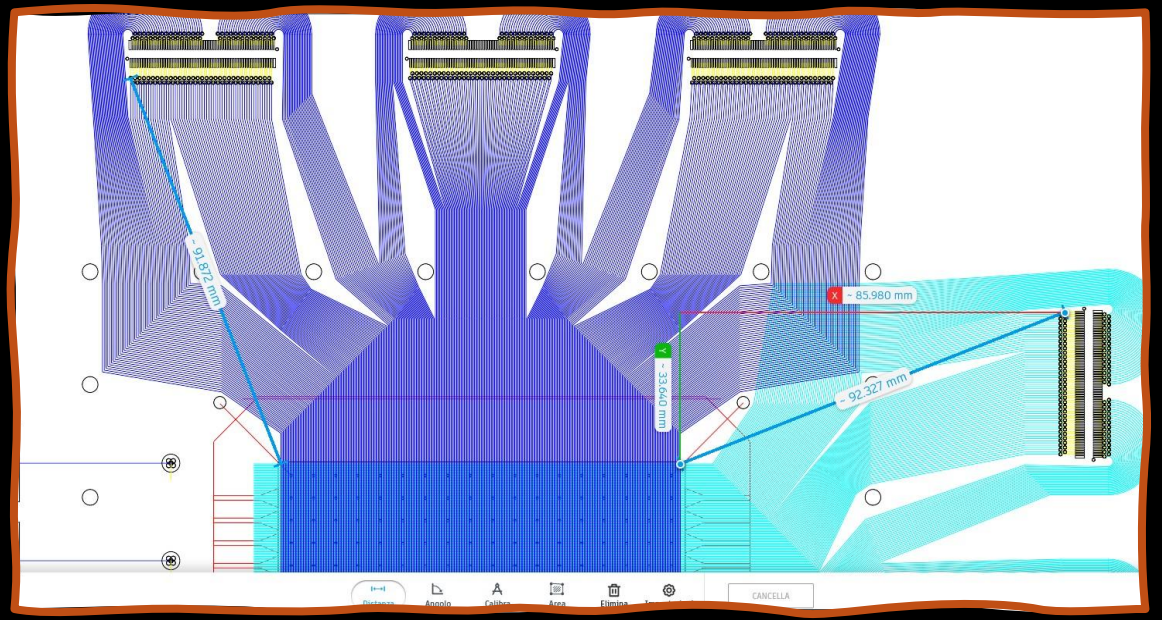

Beam Monitor